Key Points:

- Topsoil (5 cm) warming increases the CO_2:CH_4 production ratio, while warming of subsoil (40 cm) leads to lower CO_2:CH_4 production ratios
- The CO_2:CH_4 production ratio is associated with active-layer depth (ALD) due to a direct effect of ALD on CH_4 production
- Carbon was preferentially lost in form of CO_2 at wet and dry sites, but CH_4 had a higher contribution at the wet tundra site

Ratio of In Situ CO_2 to CH_4 Production and Its Environmental Controls in Polygonal Tundra Soils of Samoylov Island, Northeastern Siberia

Leonardo de A. Galera[1,2] , **Tim Eckhardt[1,2]**, **Christian Beer[1,2]** , **Eva-Maria Pfeiffer[1,2]**, and **Christian Knoblauch[1,2]**

[1]Institute of Soil Sciences, Faculty of Mathematics, Informatics and Natural Sciences, Universität Hamburg, Hamburg, Germany, [2]Center for Earth System Research and Sustainability, Universität Hamburg, Hamburg, Germany

Abstract Arctic warming causes permafrost thaw and accelerates microbial decomposition of soil organic matter (SOM) to carbon dioxide (CO_2) and methane (CH_4). The determining factors for the ratio between CO_2 and CH_4 formation are still not well understood due to scarce in situ measurements, particularly in remote Arctic regions. We quantified the CO_2:CH_4 ratios of SOM decomposition in wet and dry tundra soils by using CO_2 fluxes from clipped plots and in situ CH_4 fluxes from vegetated plots. At the water-saturated site, CO_2:CH_4 ratios decreased sharply from 95 at beginning of July to about 10 in August and September with a median of 12.2 (7.70–17.1; 25%–75% quartiles) over the whole vegetation period. When considering CH_4 oxidation, estimated to reduce in situ CH_4 fluxes by 10%–31%, even lower CO_2:CH_4 ratios were calculated (median 10.9–8.41). Active layer depth and soil temperature were the main factors controlling these ratios. Methane production was associated with subsoil (40 cm) temperature, while heterotrophic respiration was related to topsoil (5 cm) temperatures. As expected, CO_2:CH_4 ratios were substantially higher at the dry site (median 373, 292–500, 25%–75% quartiles). Both tundra types lost carbon preferentially in form of CO_2, and CH_4-C represented only 0.27% of the dry tundra total carbon loss and 6.91% of the wet tundra total carbon loss. The current study demonstrates the dynamic of in situ CO_2:CH_4 ratios from SOM decomposition and will help improve simulations of future CO_2 and CH_4 fluxes from thawing tundra soils.

Plain Language Summary Global warming causes the thaw of the permanently frozen soil in Arctic regions, exposing soil organic matter (SOM) previously frozen to decomposition, increasing the emission of carbon dioxide (CO_2) and methane (CH_4), which are greenhouse gases. It is crucial to quantify the ratio of CO_2 and CH_4 produced because CH_4 has a stronger global warming potential than CO_2. We partitioned SOM decomposition into CO_2 and CH_4 formation (CO_2:CH_4 ratios) in wet and dry tundra soils on Samoylov Island, Northeastern Siberia, and we related these ratios to environmental variables. Deeper active layer, which is the topsoil layer that freezes and thaws annually, and higher subsoil (40 cm) temperature at the interface between the active layer and the permafrost, foster CH_4 production and decrease CO_2:CH_4 ratios. Carbon was preferentially lost in form of CO_2 by the soils, but CH_4 had a larger contribution to the carbon loss in the wet tundra. Our study indicates that warming and deepening of the active layer can result in rising CH_4 production. Further understanding of in situ CO_2:CH_4 ratios from SOM decomposition will help improve simulations on future CO_2 and CH_4 fluxes from thawing tundra soils.

1. Introduction

Permafrost-affected soils contain about 1,000 Pg of soil organic carbon (SOC) in the uppermost 3 m (Mishra et al., 2021). The Arctic is experiencing one of the greatest impacts of climate change in the world (IPCC, 2022). Record high permafrost temperatures were registered in the last two decades (Biskaborn et al., 2019), leading to permafrost thaw. The microbial decomposition of thawing permafrost organic matter (OM) releases the greenhouse gases (GHG) carbon dioxide (CO_2) and methane (CH_4) (Lindroth et al., 2022; Miner et al., 2022; Schuur et al., 2015). Methane has at least a 28-fold global warming potential of CO_2 (Myhre et al., 2013). Hence, we need to understand the relative emission of CO_2 to CH_4 when permafrost-affected soils warm and permafrost thaw.

The formation of CO_2 and CH_4 from thawing permafrost has been studied most often by laboratory incubations. Using this method, a wide range (<1 to >1,000) of ratios between CO_2 and CH_4 production in permafrost-affected soils have been reported (Heslop et al., 2019; Knoblauch et al., 2018; Treat et al., 2014, 2015). This wide range

Resources: Eva-Maria Pfeiffer, Christian Knoblauch
Software: Tim Eckhardt
Supervision: Tim Eckhardt, Christian Beer, Eva-Maria Pfeiffer, Christian Knoblauch
Validation: Christian Knoblauch
Visualization: Tim Eckhardt, Christian Knoblauch
Writing – original draft: Christian Knoblauch
Writing – review & editing: Tim Eckhardt, Christian Beer, Christian Knoblauch

might be caused by differences in incubation conditions and duration, and differences in the composition of OM and microbial communities (Treat et al., 2015). Since the energy gain of methanogenesis is low in comparison to microbial processes using electron acceptors such as oxygen (O_2), nitrate, iron, and sulfate, CH_4 production is low as long as these electron acceptors are available (Bodegom & Stams, 1999). Hence, the CO_2:CH_4 ratio in incubations is not constant and may decrease with incubation time, owing to the depletion of alternative electron acceptors but also due to the establishment of an active CH_4-producing community (Knoblauch et al., 2018; Philben et al., 2020). Finally, soil incubations are generally done either under anoxic or oxic conditions, while soils, even under water-saturated conditions, are characterized by redox gradients, which may last from completely anoxic to fully oxic. Thus, incubation experiments give only limited information on CO_2 and CH_4 production under in situ conditions. One approach used to measure reliable in situ CO_2 and CH_4 production rates is to derive them from soil concentration depth profiles (Clymo & Bryant, 2008; Clymo et al., 1995), but attempts to deduce the CO_2 to CH_4 production partitioning from gas measurements resulting from soil organic matter decomposition have not been done yet.

Microbial CH_4 oxidation in soil layers that contain oxygen, such as the rhizosphere, where oxygen is leaking from the roots, or the surface soil, is further modifying the in situ CO_2:CH_4 ratio. Aerobic CH_4 oxidizing bacteria may oxidize up to 99% of produced CH_4 to CO_2 in water-saturated permafrost soils, with particularly high importance of CH_4 oxidation at sites without vascular plants (Knoblauch et al., 2015; Popp et al., 2000). The relevance of CH_4 oxidation strongly depends on CH_4 transport pathways. Methane transported by molecular diffusion through the water phase is $>10^4$ times slower than ebullition or plant-mediated transport through the gas phase in air-filled tissue. Hence CH_4 oxidation is most relevant when CH_4 moves slowly through the soil (molecular diffusion in the water phase) and lowest when rapidly transported from its production zone into the atmosphere (ebullition, plant-mediated transport) (Bastviken et al., 2008; Knoblauch et al., 2015; Whalen, 2005). Hence, the release of carbon as CO_2 or CH_4 is determined by complex interactions of the factors influencing not just their production, but also their transport.

The extensive Siberian tundra is currently underrepresented in international CH_4 emissions databases (Saunois et al., 2020). There are large uncertainties regarding the controls of CH_4 production and emission in the vast Russian Arctic tundra, and consequently the response of CH_4 emission to climate change. Permafrost acts as a barrier to drainage resulting in lakes, ponds, and wetlands, characterized by anoxic conditions and accumulation of OM. The seasonal freezing and thawing of the upper soil layer (active layer) promote the creation of patterned ground, such as polygonal structures, where the depressed centers are often water saturated while the elevated rims are drained and characterized by oxic conditions (van Huissteden, 2020). Differences in vegetation type may account for substantial variation in CH_4 and CO_2 emissions from the Arctic tundra (Cannone et al., 2016; Knoblauch et al., 2015). Due to the complexity of environmental and microbial parameters affecting CH_4 production and turnover in permafrost soils, there are still large uncertainties on how thaw-induced changes in the soil hydrology of permafrost landscapes will impact in situ CO_2 and CH_4 production from thawing permafrost OM and related GHG emissions (Euskirchen et al., 2017). A quantitative understanding of the regulation of the CO_2:CH_4 ratio is needed to improve process-based models simulating the feedback between thawing permafrost and global change. Most global models still calculate CH_4 production or emission as a fixed ratio of soil organic matter (SOM) decomposition (Kleinen et al., 2021; Melton et al., 2013; Wania et al., 2010).

The objective of this study is to improve our knowledge of the regulation of the ratio between microbial CO_2 and CH_4 production from OM decomposition under in situ conditions of a typical polygonal tundra. For this, small-scale approaches, such as chamber measurements are more appropriate than eddy-covariance systems (Krauss et al., 2016). Therefore, we used an experimental setup based on the chamber approach and measured for a whole summer season (July–September) in situ greenhouse gas fluxes at two soils of the Siberian polygonal tundra characterized by different hydrological regimes. Methane production was estimated using fluxes from plots vegetated by vascular plants, and CO_2 fluxes representing heterotrophic respiration (R_h) were quantified from clipped plots of a root-trenching experiment (Eckhardt et al., 2019). By this approach, we identified the relative contribution of CO_2 and CH_4 production during OM decomposition in permafrost-affected soils under in situ conditions, identified the most important environmental parameters regulating the in situ ratio between CO_2 and CH_4 production, and estimated the contribution of plant-mediated CH_4 transport to total CH_4 emissions. Finally, we used the obtained CO_2 and CH_4 data to calculate the production of CO_2 and CH_4 in the polygonal tundra of Samoylov Island for one summer thaw season.
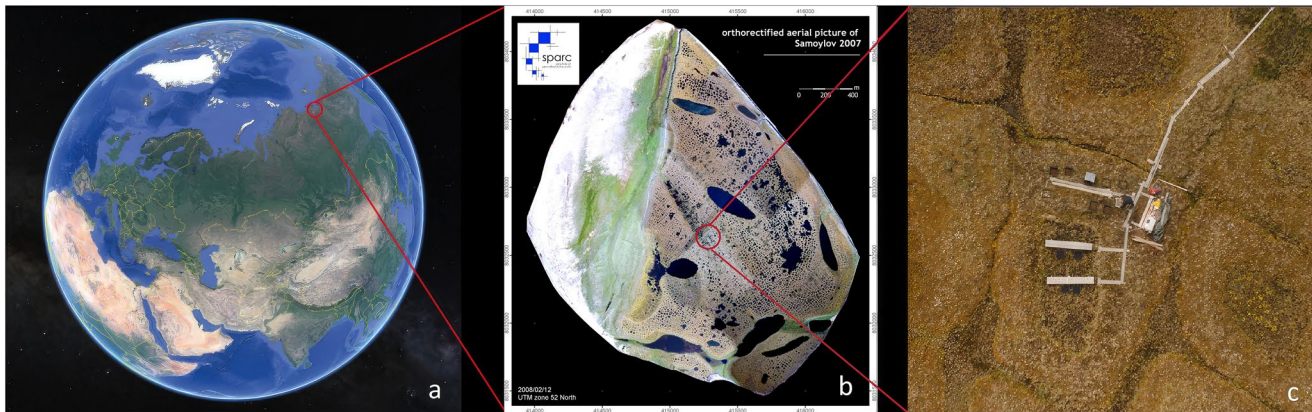
Figure 1. The study site on Samoylov Island, Lena River Delta, Northeastern Siberia (72°22′N, 126°28′E) from the perspective of the Eurasian continent. Panel (a): Eurasia (Google, n.d.); (b): Orthorectified aerial picture of Samoylov Island, Lena River Delta, Northeastern Siberia, Russia (Boike et al., 2012); (c): Studied polygon in Samoylov Island (Boike et al., 2015).

2. Material and Methods

2.1. Study Site

The study was conducted on Samoylov Island in the southern central Lena River Delta, Northeastern Siberia (72°22′N, 126°28′E) in the continuous permafrost zone, with permafrost depths of 300–500 m (Yershov, 1998) (Figure 1). The annual mean permafrost temperature is −8.6°C at about 11 m depth, while temperatures at the surface soil can vary from 20°C to −35°C throughout the year. The island has an arctic continental climate with an annual mean temperature of −12.5°C and annual mean precipitation of 321 mm (Boike et al., 2013). Snow-melt starts in June and the growing season lasts from mid-June to mid-September. Polar days, which are days when the sun remains above the horizon for 24 hr, span from 7 May to 8 August, and polar nights, which are days when the sun remains below the horizon for 24 hr, spanning from 15 November to 28 January. The study has been executed at the eastern part of Samoylov Island, which is covered by ice-wedge polygonal tundra on a Late Holocene river terrace, characterized by ice-rich alluvial deposits. The polygonal tundra is formed by depressed polygon centers surrounded by elevated polygon rims with an elevation difference of about 0.5 m. Water-saturated soils are often found in the polygon centers due to the underlying permafrost that prevents drainage while soils at the elevated polygon rims are well-drained. Mean carbon pools in the uppermost 1 m are higher in the polygon centers (33 kg SOC m^{-2}) than in the polygon rims (19 kg SOC m^{-2}) (Zubrzycki et al., 2013).

The study was carried out in a polygon (72°22′26″N, 126°29′49″E) with one sub-site in the water-saturated, depressed polygon center (wet tundra) and another sub-site in its surrounding polygon rim (dry tundra). The soil at the polygon center was classified as Reductaquic Cryosol (WRB, 2015) with the water table varying from 7 cm below to 7 cm above the soil surface during the measurement period, a maximum yearly active layer depth (ALD) of 40 cm and vegetation dominated by mosses (*Drepanocladus revolvens*, *Meesia triqueta*, *Scorpidium scorpioides*) and the hydrophilic sedge *Carex aquatilis*. Total organic carbon (TOC) concentrations in the polygon center soil ranged between 10.1% and 19.6%, with the highest concentrations in the uppermost 6 cm (Figure S1 in Supporting Information S1). The soil at the polygon rim was classified as Turbic Glacic Cryosol (WRB, 2015) with the water table a few centimeters above the permafrost table, maximum ALD of 30 cm, and vegetation dominated by mosses (*Hylocomium splendens*, *Polytrichum spp.*, *Rhytidium rugosum*), some small vascular plants (*Dryas punctata* and *Astragalus frigidus*) and lichens (*Peltigera spp.*). The polygon rim soil contained 12.3% of TOC in the uppermost 15 cm depth and cryoturbated horizons bellow 15 cm (Figure S2 in Supporting Information S1).

2.2. Soils and Meteorological Data

The soil temperatures (Soil*T*) at 2, 5, 10, 15, and 40 cm and air temperature (Air*T*) at 2 m height, precipitation, and incoming and outgoing components of shortwave and longwave radiation were recorded by a nearby

meteorological station in the center and rim of a similar polygon about 40 m southwest of the study site (Boike et al., 2019). The surface temperature (Surf$T$) was estimated by the following equation:

$$\text{Surf}T = \left(\frac{L\uparrow_{\text{B}}}{\varepsilon\sigma} \right)^{\frac{1}{4}} \tag{1}$$

where $L\uparrow_{\text{B}}$ is the upward infrared radiation (W m^{-2}), ε is the dimensionless emissivity with a value of 0.98 and σ is the Stefan-Boltzmann constant (W m^{-2} K^{-4}) (Wilber et al., 1999). The Surf$T$ was calculated in Kelvin with Equation 1 and converted to degrees Celsius.

The description of the water table depth (WT) measurements in the center, the volumetric soil water content (VWC) at the rim, and the ALD in both sub-sites can be found in Eckhardt et al. (2019).

2.3. Chamber Measurements and Plant-Mediated CH$_4$ Transport

At each sub-site, 10 measurement plots made of PVC frames (50 × 50 cm) were established. From these, four had their original vegetation intact (hereafter called "vegetated"), while six had the surface vegetation removed (hereafter called "clipped"). The experiment has been described in detail by Eckhardt et al. (2019). The frames were inserted 20 cm deep into the soil, below the main rooting zone. The opaque acrylic chamber was equipped with a fan for the mixing of the air. The chambers were 50 cm high and enclosed a volume between 124 and 143 L, depending on the terrain inside the chamber frames. Two holes with 3 cm of diameter were left open at the top of the chamber while placing it slowly on the frames to avoid pressure-induced gas release from the soil (Christiansen et al., 2011; Eckhardt et al., 2019). These holes were closed before the measurement. A boardwalk was installed at the polygon to avoid disturbances. We performed a clipping experiment by using the root-trenching method in four frames at each sub-site on the polygon (center and rim) in 2014. In addition to the cutting of the lateral roots through the insertion of the PVC frames, all living plant biomass, including mosses, was carefully removed from within the "clipped" frames. During the measurement period in 2015, this procedure was repeated periodically to prevent plant regrowth. Additionally, two frames were installed in 2015 and clipped at each sub-site to test if CO$_2$ fluxes were biased due to the additional decomposition of residual roots, which might be a possible artifact of the root-trenching method. However, no significant difference between the CO$_2$ fluxes in the clipped plots of 2014 and those clipped in 2015 was observed (Eckhardt et al., 2019).

The CH$_4$ concentrations in the headspace of the chambers were measured with a portable gas analyzer (UGGA 30-p; Los Gatos Research, USA) and recorded with a data logger (CR800 series; Campbell Scientific Ltd., USA). The precision of the gas analyzer for CH$_4$ is better than 0.005 ppm. Chamber closure time was 120 s, during which chamber headspace air was pumped in a closed loop through the analyzer at a rate of 200 mL min^{-1}. The chamber closure of 120 s was chosen to prevent the warming inside the chamber in relation to the exterior temperature. This amount of time was sufficient for the detection of small CH$_4$ concentration variations in the headspace while averting its temperature increase. Measurements were conducted between 11 July and 22 September, 2015, except in the periods between 2 and 9 August, when a shift change between researchers took longer than expected, and the 17 and 24 August, when the measurements were impossible due to a heavy storm event. During the measurement period, measurements were taken at least every third day. The R_h fluxes used in this study are from Eckhardt et al. (2019). The CH$_4$ fluxes were calculated using MATLAB (R2019a. In The MathWorks Inc.) with a routine combining different regression models, such as linear, exponential, and increasing polynomial degrees, and statistical analysis for model selection. Details can be found in Eckhardt and Kutzbach (2016). Methane concentrations inside the chamber headspace increased linearly over time (Figure S3 in Supporting Information S1), thus linear regressions have been used for the flux calculation. The first 30 s of each 120 s measurement period were discarded to eliminate possible perturbations when placing the chamber on the frame. The fraction of plant-mediated CH$_4$ fluxes was calculated as the difference between the daily mean CH$_4$ fluxes from the vegetated plots and the clipped plots (Table 1).

2.4. Calculation of CO$_2$:CH$_4$ Ratios and Uncertainty Range

The CO$_2$:CH$_4$ ratios were calculated on a molar basis, using the daily mean CH$_4$ fluxes from the vegetated plots, and the daily mean R_h fluxes, which were measured with dark chambers in the clipped plots (see Eckhardt

Table 1

Median (in Bold), First (Q1), and Third (Q3) Quartiles of CH$_4$ Fluxes During the Growing Season of 2015 From Vegetated and Clipped Plots in a Polygon Center and a Polygon Rim on Samoylov Island, and Contribution of Plant-Mediated CH$_4$ Transport

| | CH$_4$ flux (mg m^{-2} d^{-1}) | | | | | | Plant-mediated transport (%) | | |
| | Vegetated | | | Clipped | | | | | |
Polygon sub-site	Q1	Median	Q3	Q1	Median	Q3		Q1	Q3
Center	21.1	**26.4**	32.5	2.63	**4.31**	9.19	65.3	**79.3**	89.3
Rim	1.58	**1.85**	2.20	1.50	**1.67**	1.91	−15.7	**2.86**	20.9

et al., 2019). The CH$_4$ fluxes above vegetated plots in the water-saturated polygon center are the best estimate of in situ CH$_4$ production. These fluxes might underestimate the CH$_4$ production since no CH$_4$ oxidation is considered. However, we have estimated the range of CH$_4$ oxidation that could be affecting our measured fluxes using the fraction of oxidized CH$_4$ and plant-mediated CH$_4$ transport data from studies in sites similar to this study, as is described later in this section. Hence, the calculated CO$_2$:CH$_4$ ratios of the polygon center are considered the CO$_2$:CH$_4$ production ratios. However, this is not the case for CH$_4$ fluxes from the polygon rim due to high CH$_4$ oxidation in the unsaturated soil. This procedure resulted in one single CO$_2$:CH$_4$ ratio per day in each sub-site on the polygon center and rim. Thus, to obtain a variation measure for these daily ratios, we propagated the standard deviation of the CH$_4$ and CO$_2$ daily fluxes using the following equation (Singh & Chaturvedi, 2021):

$$\sigma_{CO2:CH4} = \sqrt{\left(\frac{\sigma_{CO2}}{f_{CO2}}\right)^2 + \left(\frac{\sigma_{CH4}}{f_{CH4}}\right)^2} \, x \, CO_2:CH_4 \qquad (2)$$

where $\sigma_{CO2:CH4}$ is the estimated standard deviation of the CO$_2$:CH$_4$ ratio; CO$_2$:CH$_4$ is the mean CO$_2$:CH$_4$ ratio; σ_{CO2} is the standard deviation of the CO$_2$ fluxes; f_{CO2} is the mean CO$_2$ flux; σ_{CH4} is the standard deviation of the CH$_4$ fluxes and f_{CH4} is the mean CH$_4$ flux.

Our approach to estimating CH$_4$ production in the soil from CH$_4$ fluxes above vegetated plots is neglecting CH$_4$ oxidation in the soil, which causes an underestimation of in situ CH$_4$ production. To account for this potential error, we used published data on CH$_4$ oxidation (Knoblauch et al., 2015; Preuss et al., 2013) at water-saturated polygon centers on Samoylov that were vegetated by the same vascular plant (*Carex aquatilis*) as our site (Table 2). The polygon center daily average CH$_4$ fluxes ($f_{CH4(corrected)}$) were recalculated as follows:

$$f_{CH4(corrected)} = \left(\frac{D_{CH4}}{1 - MOR} + P_{CH4}\right) x \, f_{CH4} \qquad (3)$$

where MOR is the fraction of produced CH$_4$ oxidized in the soil, D_{CH4} is the fraction of CH$_4$ transported through the soil, P_{CH4} is the fraction of CH$_4$ transported through plants and f_{CH4} is the mean CH$_4$ flux. The MOR values were retrieved from the literature, and the D_{CH4} values were either CH$_4$ fluxes from the clipped plots of this study or additional values retrieved from the literature. The use of these values in the definition of the upper and lower boundaries of the uncertainty range is shown in Table 2. The lower boundary uses the lowest CH$_4$ oxidation from

Table 2

Fraction of CH$_4$ Transported Through the Bulk Soil (D$_{CH4}$) and of Plant-Mediated Transport (P$_{CH4}$) as Well as CH$_4$ Oxidized in Water-Saturated Polygon Centers, Vegetated by Carex aquatilis on Samoylov Island

Study	Fraction P_{CH4}	Fraction D_{CH4}	Fraction of CH$_4$ oxidized in bulk soil	Fraction of total CH$_4$ oxidized	CH$_4$ production (mg CH$_4$ m^{-2} d^{-1})	CO$_2$:CH$_4$ production ratio
Assumption 1 (no CH$_4$ oxidation)	0.79[a]	0.21[a]	0	0	26.4 (21.1–32.5)	12.2 (7.70–17.1)
Assumption 2 (lowest CH$_4$ oxidation, highest P_{CH4})	0.86[b]	0.14[b]	0.45[c]	0.10	29.5 (23.5–36.3)	10.9 (6.91–15.4)
Assumption 3 (highest CH$_4$ oxidation, lowest P_{CH4})	0.79[a]	0.21[a]	0.68[b]	0.31	38.2 (30.5–47.1)	8.41 (5.32–11.8)

Note. Methane production and CO$_2$:CH$_4$ production ratios are calculated for three assumptions regarding the fraction of CH$_4$ oxidized and of the different transport pathways (see Section 2, Equation 3).
[a]This study. [b]Knoblauch et al. (2015). [c]Preuss et al. (2013).

Table 3

Heterotrophic Respiration (R_h) Measured With Dark Chambers in Clipped Plots and CH_4 Fluxes Measured With Transparent Chambers in Vegetated Plots From Two Sub-Sites in the Polygonal Tundra on Samoylov Island During the Growing Season in 2015

GHG	kg ha^{-1} d^{-1}	kg-C ha^{-1} d^{-1}	Area	kg-C d^{-1}	% of total C fluxes
Wet tundra					
CO_2 (R_H)	9.81	2.68	×54.1 ha	145	93.1
CH_4	0.265	0.199	×54.1 ha	11	6.91
Total		2.87		155	100
Dry tundra					
CO_2 (R_H)	19.5	5.32	×185 ha	984	99.7
CH_4	0.019	0.014	×185 ha	3	0.27
Total		5.33		986	100

Note. The table shows the median fluxes calculated after gap-filling by linear interpolation (see Methods). Both fluxes were converted to carbon mass to allow a direct comparison between them. Moreover, both fluxes were multiplied by the wet and dry tundra area (in italic) (Muster et al., 2012) to calculate the seasonal R_h and CH_4 release for the whole polygonal tundra of Samoylov Island. R_h data are from Eckhardt et al. (2019). The last column shows the contribution of each GHG in total C fluxes.

Preuss et al. (2013), and the highest P_{CH4} from Knoblauch et al. (2015). The upper boundary uses the highest CH_4 oxidation from Knoblauch et al. (2015) and the lowest $P_{CH4,}$ which was found in this study. This approach assumes that only CH_4 diffusing slowly through the soil is affected by CH_4 oxidation but not that fraction of CH_4, which is released rapidly by plant-mediated transport. These new daily mean CH_4 fluxes were then used to recalculate the center CO_2:CH_4 production ratios as described above.

2.5. Calculation of the Seasonal Heterotrophic Respiration and CH_4 fluxes

The seasonal R_h and CH_4 fluxes were calculated from the CO_2 of clipped plots and CH_4 fluxes of vegetated plots of the wet (polygon center) and dry tundra (polygon rim) in kilograms per hectare per day, during the measurement period. The daily average R_h fluxes of the clipped plots measured with the dark chamber, representing the R_h, were taken from Eckhardt et al. (2019). From 11 July 2015 to 22 September 2015 there were 47 days with R_h and CH_4 measurements. We filled the gaps between measurements by linearly interpolating the daily average of R_h and CH_4 fluxes (W. Chen et al., 2011; Khokhar & Park, 2017; Kwon et al., 2017; Natchimuthu et al., 2017; Schrier-Uijl et al., 2010; Wickland et al., 2006). For the direct comparison of R_h and CH_4 fluxes (Table 3), the median R_h fluxes and the median CH_4 fluxes were normalized to carbon (kg CO_2-C/CH_4-C ha^{-1} d^{-1}) to consider the mass differences between the two molecules. For the comparison based on the whole area of Samoylov (Table 3), we used the fraction of wet and dry tundra (19% and 65%, respectively) of the polygonal tundra mapped by Muster et al. (2012) on Samoylov Island, resulting in 54 ha of wet tundra and 185 ha of dry tundra. The active floodplains and open water bodies have not been included in our study. The CO_2-C and CH_4-C fluxes were multiplied by the area of each land cover (dry and wet tundra), resulting in daily absolute CO_2-C and CH_4-C production (kg CO_2-C/CH_4-C d^{-1}) of each tundra type.

2.6. Statistics

The CO_2:CH_4 ratios of the polygon center and rim were analyzed separately through linear regression models. First, we have tested the relationship between CO_2:CH_4 ratios and each of the daily mean environmental variables, namely soil temperatures at 2 cm, 5 cm (Soil$T$5), 10, 15, and 40 cm depth (Soil$T$40), Surf$T$, ALD, WT (for the polygon center) and VWC (for the polygon rim) and selected the best predictors. The same was made with the CH_4 and R_h daily mean fluxes, to test the relationships between the predictors and the CO_2:CH_4 ratios. Natural logarithm transformation was applied for non-normally distributed data.

Then, a multivariate regression model relating the CO_2:CH_4 ratios with the best predictors, chosen during the abovementioned linear regressions between CO_2:CH_4 ratios and individual environmental parameters, was set including the possible interaction between predictors. If the interaction between predictors was not significant ($p > 0.05$), the sum of their effects was considered. The possibility of logarithmic and exponential relationships between response variables and predictors was also verified throughout the previous steps.

We chose the model with the highest R^2, smallest root mean squared error (RMSE), lowest p-value from the model F-test ($\alpha = 0.05$), and the lowest Akaike Information Criterion (AIC) that gives the relative quality of statistical models for the same data set. The best-adjusted regressions are shown in the results section. The statistical analyses were performed in R (R, 2020).

3. Results

3.1. CH_4 Fluxes and Plant-Mediated Transport

The CH_4 fluxes from the vegetated plots at the polygon center varied throughout the measurement period, showing a clear seasonality (Figure 2). There was a fast increase in July, at the beginning of the growing season,
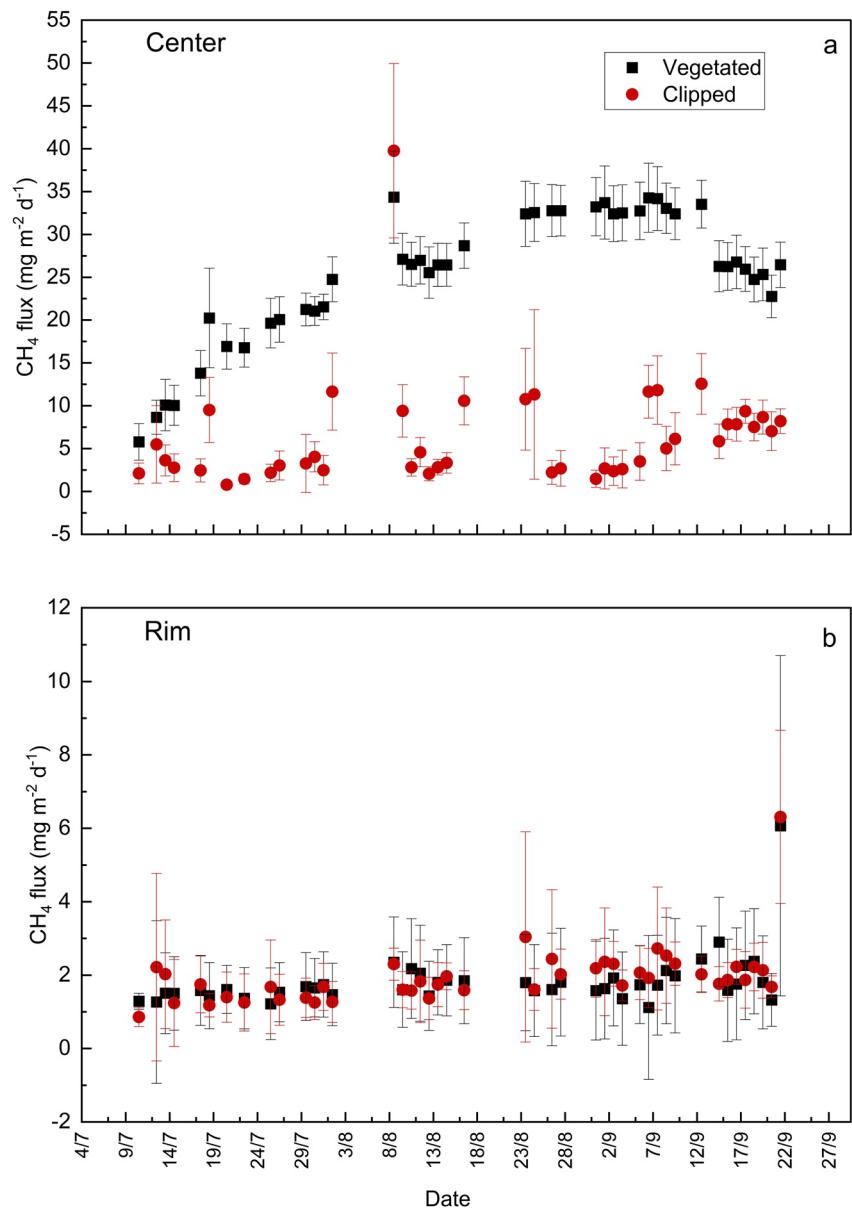
Figure 2. Daily mean and standard deviation of CH_4 fluxes ($n = 8$) between July and September 2015 from a polygon on Samoylov Island at vegetated and clipped plots in the polygon center (a) and polygon rim (b).

followed by a slower increase in the first weeks of August. The fluxes stabilized at the peak rates, representing six times the flux measured at the beginning of July, from mid-August until the beginning of September, when the fluxes started to decrease at the end of the growing season. The variation of CH_4 fluxes at the polygon rim showed no seasonality but a sudden increase on the 22nd of September, the last day of measurements.

The median CH_4 flux of the vegetated plots at the polygon center was 26.4 mg $m^{-2}d^{-1}$ (21.1–32.5 mg m^{-2} d^{-1}; 25%–75% quartiles). The median CH_4 flux at the polygon rim was 1.85 mg m^{-2} d^{-1} (1.58–2.22 mg m^{-2} d^{-1}; 25%–75% quartiles). The daily CH_4 fluxes means at the center were between 3.9 and 20.2 times higher than at the rim throughout the season. The log-transformed CH_4 fluxes from vegetated plots at the center had significant relationships with the ALD ($R^2 = 0.73$; $p < 0.001$), with the SoilT40 ($R^2 = 0.68$; $p < 0.001$) and had no relationship with the SurfT ($p = 0.172$). The log-transformed CH_4 fluxes at the rim also had a significant relationship with the ALD but with a lower R^2 ($R^2 = 0.44$; $p < 0.001$) and with the SoilT40 ($R^2 = 0.42$; $p < 0.001$), but no relationship with shallower soil temperatures like the SoilT5 ($p = 0.404$) and SurfT ($p = 0.824$).
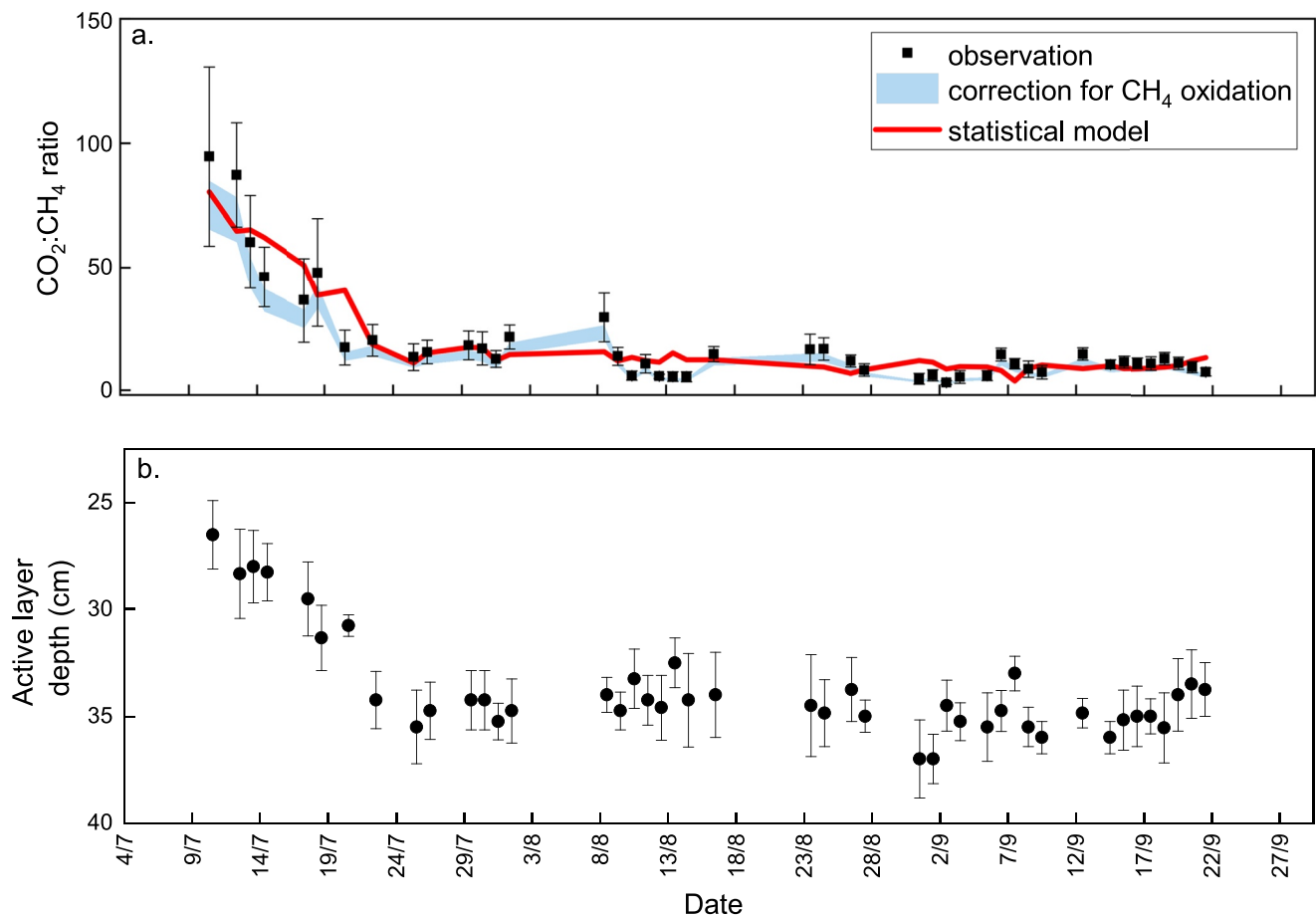
Figure 3. (a) Ratio of daily R_h fluxes from heterotrophic respiration and CH_4 fluxes at the polygon center (black squares), range of CO_2:CH_4 ratios after considering a fraction of produced CH_4 oxidized between 0.10 and 0.30 (shaded area) and results from multivariate regression analysis with active layer depth (ALD) and soil temperature at 40 cm as influence parameters (red line). Error bars give the propagated standard deviation (see Section 2.4). (b) Mean daily ALD ($n = 3$–20) at the polygon center during the growing season in 2015. Errors bars are standard deviation.

The mean daily CH_4 fluxes of the clipped plots at the polygon center were lower than those from the vegetated plots. The differences between vegetated and clipped plots are smaller at the beginning of the growing season compared to later periods. Based on the differences in CH_4 fluxes between clipped and vegetated plots, the median plant-mediated CH_4 transport at the polygon center is 79% (65%–89%, 25%–75% quartiles). At the polygon rim, there was only a very small difference between clipped and vegetated plots of 3% (Table 1).

Based on stable isotope signatures of CH_4 dissolved in the water-saturated soil of polygon centers on Samoylov, it has been estimated that a fraction between 0.45 and 0.68 of the CH_4 diffusing through the bulk soil is oxidized to CO_2 before emitted into the atmosphere (Knoblauch et al., 2015; Preuss et al., 2013) (Table 2). Using this range of CH_4 oxidation and the fraction of plant-mediated CH_4 transport (P_{CH4}) and CH_4 transport through the bulk soil (D_{CH4}) determined in this and previous studies (Knoblauch et al., 2015; Preuss et al., 2013) we calculated that a fraction between 0.10 and 0.31 of produced CH_4 might have been oxidized before emitted into the atmosphere (assumptions 2 and 3, Table 2). Using these CH_4 oxidation estimates would increase the median of CH_4 production rates from 26.4 mg m^{-2}d^{-1} (no oxidation assumed) to 29.5 mg m^{-2}d^{-1} (fraction of 0.10 oxidized) and 38.2 mg m^{-2}d^{-1} (fraction of 0.31 oxidized) (Table 2).

3.2. CO_2:CH_4 Ratios, Their Environmental Controls, and Uncertainty Range

The CO_2:CH_4 ratios, calculated from in situ CH_4 fluxes from vegetated plots and R_h, varied between 3 and 95 at the polygon center (Figure 3), while they varied at the rim between 80 and 1,074. The CO_2:CH_4 ratios at the polygon center were around 95 at the beginning of July and decreased rapidly until mid-July. From 21 July on, the

Table 4
Statistical Models Describing the Relationship Between CO_2:CH_4 Ratios and Environmental Variables, Selected According to Criteria Described in the Methods Section (See Section 2.6)

Sub-site	Center	Rim
Statistical model	CO_2:$CH_4 = -0.811(ALD) - 174(logSoilT40) + 4.79\ (ALD*logSoilT40) + 40.6$	CO_2:$CH_4 = 29.9(SoilT5) - 7.84(ALD) + 446$
R^2	0.88	0.63
p-value	<0.001	<0.001
RMSE	6.86	103
Interaction	significant ($p < 0.001$)	not significant ($p = 0.459$)

Note. "Interaction" states the interaction between predictors.

ratios ranged between 7 and 15. There was a high variability of CO_2:CH_4 ratios in the polygon rim. The amplitude of this variation and the ratios themselves are higher in July and steadily decrease over time. From 12 September on, this downward trend is seen more clearly (Figure S7 in Supporting Information S1). The median CO_2:CH_4 ratio was 12.2 (7.70–17.1; 25%–75% quartiles) at the polygon center and 373 (292–500, 25%–75% quartiles) at the polygon rim.

The best predictor of the CO_2:CH_4 ratios at the polygon center was the ALD, with a linear relationship ($R^2 = 0.72$; $p < 0.001$) (Figure 3). Both the CO_2:CH_4 ratio and the ALD stabilize around a constant value from the end of July until the 22 September. The second-best predictor for the CO_2:CH_4 ratios at the polygon center was the SoilT40 with a logarithmic relationship ($R^2 = 0.65$; $p < 0.001$). The center CO_2:CH_4 ratios have exponential relationships with AirT ($R^2 = 0.36$; $p < 0.001$) and SurfT ($R^2 = 0.35$; $p < 0.001$).

The CO_2:CH_4 ratios at the polygon rim had higher variability and a more gradual decreasing trend along the season than at the center. The best predictors of the CO_2:CH_4 ratios at the polygon rim were the SoilT5 (lin; $R^2 = 0.55$; $p < 0.001$) and the SurfT (lin; $R^2 = 0.45$; $p < 0.001$). However, the inclusion of the SurfT as a predictor along with the SoilT5 into the multivariate regression model did not add explanatory power to it due to collinearity, which was shown by a higher AIC. For that reason, the ALD, which was the third best predictor (lin; $R^2 = 0.30$; $p < 0.001$), was included instead, with a significant increase in the quality of the model ($p = 0.024$). The statistical models that showed the best explanatory power for the CO_2:CH_4 ratios at the polygon center and rim are shown in Table 4.

In addition to the relationships between R_h and environmental variables reported by Eckhardt et al. (2019), we present here some additional relationships that improve our understanding of the CO_2:CH_4 ratios. The R_h at the polygon center showed relationships with the SurfT (lin; $R^2 = 0.59$; $p < 0.001$), with the SoilT40 (log; $R^2 = 0.24$; $p < 0.001$) and no relationship with the ALD (lin; $p = 0.062$). The R_h at the polygon rim had a linear relationship with the SoilT5 ($R^2 = 0.60$; $p < 0.001$) but none with the ALD (lin; $p = 0.076$). Furthermore, there was a weak linear relationship between the SurfT and the SoilT40 at the polygon center ($R^2 = 0.1305$; $p = 0.016$).

Using CH_4 fluxes corrected for CH_4 oxidation ($f_{CH4(corrected)}$) to calculate ratios between CO_2 and CH_4 production results in a decrease in CO_2:CH_4 ratios (Figure 3) with median values of 10.9 (fraction of 0.10 oxidized) and 8.41 (fraction of 0.31 oxidized) in comparison to 12.2 (no oxidation assumed) (Table 2).

3.3. Seasonal Heterotrophic Respiration and CH_4 fluxes

The median R_h, which was measured with the dark chamber in the clipped plots, of the wet tundra during the thaw season was lower than the one of the dry tundra's, while the median CH_4 flux, which was measured with the transparent chamber in the vegetated plots, of the wet tundra, was higher than of the dry tundra (Table 3). The R_h and CH_4 fluxes were converted to kg-C fluxes to allow a direct comparison between them. The wet tundra, although releasing more CH_4 than the dry tundra, emitted around half the total kg-C of the dry tundra. When the size of each land cover is considered, the dry tundra emits more than six times the total kg-C, as R_h and CH_4, of the wet tundra. Due to the small area of wet tundra on Samoylov Island and the low contribution of CH_4 to the dry tundra GHG fluxes, CH_4 contributed only 1.17% (or 13.4 kg-C d^{-1}) to the total daily flux of carbon from the polygonal tundra on Samoylov (1,142 kg-C d^{-1}, Table 3).

4. Discussion

4.1. CH$_4$ Fluxes in Comparison to Other Arctic Sites

The median CH$_4$ fluxes from the vegetated plots during the growing season from the polygon center in this study (26.4 mg m^{-2} d^{-1}) are at the lower end of CH$_4$ fluxes reported from the water-saturated polygonal tundra on Samoylov vegetated by vascular plants of 28.0—100.0 mg m^{-2} d^{-1} (Knoblauch et al., 2015; Kutzbach et al., 2004; Sachs et al., 2010; D. Wagner et al., 2003). These differences can be related to the high spatial and temporal variability of CH$_4$ fluxes in the Siberian tundra (Skeeter et al., 2020), but also to differences in CH$_4$ flux calculation. The highest CH$_4$ flux from water-saturated polygon centers on Samoylov (77.9—100.0 mg m^{-2} d^{-1} [Sachs et al., 2010]) was calculated from an initial non-linear CH$_4$ concentration increase with an exponential model, resulting in higher fluxes than linear models. We could only observe an initial non-linear rise of CH$_4$ concentrations after inducing a pressure increase inside the chamber when placing it on the frames. Under standard measurement conditions, CH$_4$ concentrations increased linearly inside the chambers (Figure S3 in Supporting Information S1). Hence, we used a linear fit to calculate CH$_4$ fluxes. Also, median CH$_4$ fluxes from the dry polygon rim (1.85 mg m^{-2} d^{-1}) were lower than from previous measurements (4.3–4.9 mg m^{-2} d^{-1}) (Kutzbach et al., 2004; Sachs et al., 2010; D. Wagner et al., 2003) but, as expected, all studies showed substantially lower fluxes from the dry rim than from the wet centers. Eddy covariance CH$_4$ measurements from a representative mix of wet and dry tundra, with some stretches of open water from Samoylov Island, are a good baseline reference for our results. Our median polygon center CH$_4$ fluxes (26.4 mg m^{-2} d^{-1}) are still higher than the growing season median CH$_4$ fluxes in Samoylov Island from 2014 (14.3 mg m^{-2} d^{-1}) (Beckebanze, Runkle, et al., 2022) and 2019 (16.7 mg m^{-2} d^{-1}) (Beckebanze, Rehder, et al., 2022), while our polygon rim median CH$_4$ fluxes (1.85 mg m^{-2} d^{-1}) was still lower than the fluxes of these representative areas of the polygonal tundra on the island.

Methane fluxes from the water-saturated polygon center of our study site are also at the lower end compared to other Arctic tundra soils. Studies in the Arctic report CH$_4$ fluxes in wet tundra environments ranging between 1.53 and 419 mg CH$_4$ m^{-2} d^{-1} (Andresen et al., 2017; Kwon et al., 2017; Skeeter et al., 2020; Ström et al., 2012; Vasiliev et al., 2019; I. Wagner et al., 2019). Most studies on Arctic CH$_4$ fluxes report data from organic soils, which are characterized by the highest CH$_4$ fluxes (Andresen et al., 2017; Kwon et al., 2017; Ström et al., 2012), mainly when supported by a dense cover of vascular plants like *Eriophorum* sp., *Carex* sp. or *Arctophila* sp. (Andresen et al., 2017; Ström et al., 2012). The CH$_4$ fluxes found in this study are high if only compared to mineral soil wetlands (Skeeter et al., 2020; Vasiliev et al., 2019; I. Wagner et al., 2019). The soils of both polygon center and rim in our study are mineral soils with a sandy texture (Eckhardt et al., 2019), and lower CH$_4$ fluxes from mineral soils than from organic soils have been reported in previous studies (Christiansen et al., 2015). Moreover, the Lena River Delta is one of the coldest permafrost regions on Earth (Romanovsky et al., 2010) and methanogenesis is largely controlled by temperature (Yvon-Durocher et al., 2014).

The unusually high CH$_4$ fluxes measured on 9 August, coincided with the second hottest day of the season, only after 13 July. The average AirT was 17.1°C, and the average SurfT was 21.3°C. The temperature of the methane-producing layer in the soil at around 40 cm depth on 9 August was −0.1°C on average, which was the last day of negative temperatures measured at this depth during the season. This "zero curtain" period of this specific soil layer could explain the high fluxes since CH$_4$ trapped in the soil could have been released during thawing. Although 13 July was hotter (average air temperature of 18°C), CH$_4$ fluxes were much lower because the active layer was not as deep as on 9 August, and the soil temperature at 40 cm depth was −0.7°C, the second lowest temperature at this depth after 12 July.

As expected, the CH$_4$ fluxes at the drained polygon rim in our study were very low and less variable than at the wet polygon center sub-site, however, it did not act as a CH$_4$ sink, as reported in other studies (Jørgensen et al., 2015; Kwon et al., 2017; Skeeter et al., 2020; St Pierre et al., 2019). The lack of water saturation and consequently oxic conditions demonstrated by the VWC, which varied from 28.1% to 31.8% within the study period, is probably the main reason for the lower CH$_4$ fluxes detected at the rim compared to the center. In contrast to the polygon center, water saturation was never achieved at the polygon rim, reducing the habitat for methanogens to produce CH$_4$, and setting the conditions for methanotrophs to oxidize CH$_4$. The CH$_4$ fluxes of the polygon center showed a gradual increase over the first part of the growing season until a peak and posterior decrease, while constant CH$_4$ fluxes were measured at the polygon rim. These patterns were very similar to those reported by D. Wagner et al. (2003), although, differently than here, the center CH$_4$ fluxes reached the peak earlier in mid-July, when

they started to decrease continuously. D. Wagner et al. (2003) related the seasonal fluctuations to the microbiological processes of CH_4 production and oxidation, with higher CH_4 production and lower CH_4 oxidation in the early summer and the opposite by the end of the season. The same seasonality trends of polygon center and rim CH_4 fluxes can be found in other regions in Northeastern Siberia (Kwon et al., 2017), as well as in other Arctic environments (Ström et al., 2012). Physical environmental parameters such as surface temperature (Pickett-Heaps et al., 2011) and soil temperature (Delwiche et al., 2021) have been pointed out as strong predictors of seasonal CH_4 variability. Seasonal vegetation patterns are also playing a crucial role in CH_4 seasonality. Evidence in the literature shows a strong correlation between peak season CH_4 fluxes and maximum gross ecosystem production (Nielsen, Michelsen, Strobel, et al., 2017) and between the development of the vegetation root system along the growing season and CH_4 fluxes (Joabsson & Christensen, 2001). Yet, inter-annual CH_4 fluxes variation can be significant, with largely different seasonal patterns found between years (Mastepanov et al., 2013).

Despite the absence of seasonality in the variation of CH_4 fluxes at the polygon rim, anomalously high CH_4 fluxes were measured there on the 22 September, the last day of measurements. The 22 September was also the only day of the campaign in which negative soil temperatures were recorded at 2 cm depth, indicating that the soil profile was becoming completely frozen since negative temperatures were already being recorded at and below 5 cm. We hypothesize that CH_4 stored at soil and vegetation cavities was being squeezed out to the atmosphere during the zero curtain period, in which the soil layer between the freezing top and permafrost remains unfrozen at around 0°C for months. Previous studies showed similar results with a strong soil gas pressure increase (Tagesson et al., 2012) and CH_4 fluxes increase (Mastepanov et al., 2008; Pirk et al., 2015; Zona et al., 2016) as the soil started to freeze in fall.

4.2. Impact of Plant-Mediated CH_4 Transport

The importance of plant-mediated CH_4 transport in wetlands has been documented in previous studies and mainly depends on plant type and density (Knoblauch et al., 2015; Popp et al., 2000). Plants enhance CH_4 release by facilitating CH_4 transport from the soil into the atmosphere through air-filled plant tissue (aerenchyma) and also support CH_4 production by the release of root exudates, which fuel methanogenesis in the anoxic soil (Girkin et al., 2018). The seasonality of the difference between CH_4 fluxes from clipped and vegetated plots in our study is characterized by a smaller difference between treatments at the beginning of the growing season and a gradual increase of the difference until mid-September when the difference starts to decrease again. Notwithstanding, Noyce et al. (2014) showed, in a similar clipping experiment, that the largest difference between clipped and vegetated sites occurred during fall when sedges were senescing. The authors hypothesized that a higher water table in fall kept the rooting zone saturated, intensifying the root's influence on CH_4 production and transport. This was not the case in our measurements in September, as the water table depths were at the lowest level since the start of the measurements in July (Eckhardt et al., 2019), therefore keeping a smaller volume of the rooting zone saturated.

The plant-mediated CH_4 transport in the polygon center (79%) is within the range of 66%–98% reported for wet sub-Arctic and Arctic tundra sites dominated by sedges and grasses (Knoblauch et al., 2015; Kutzbach et al., 2004; Morrissey & Livingston, 1992; Nielsen, Michelsen, Strobel, et al., 2017). The growth of aerenchymatous plants in Arctic sedge-dominated sites is a key factor linking CH_4 production with CH_4 fluxes to the atmosphere. Nielsen, Michelsen, Strobel, et al. (2017) identified a decoupling between peak dissolved CH_4 in the soil solution and peak CH_4 fluxes, suggesting that substrate availability of CH_4 was not the only factor controlling CH_4 fluxes. Moreover, they identified a connection between the peak gross ecosystem production and peak CH_4 fluxes indicating the importance of aerenchymatous plants in the transport of CH_4 to the atmosphere.

However, it is important to notice that the contribution of plant-mediated CH_4 transport to total CH_4 fluxes calculated from the clipping experiment is a conservative estimate. At the vegetated plots, the produced CH_4 is released rapidly through the plants into the atmosphere, thereby by-passing the oxidative layer of the soil, while some produced CH_4 is transported by soil diffusion. After clipping, the CH_4 that was once transported via the vegetation is diffusing through the water-saturated soil. Likely, a part of the produced CH_4 that would have been transported via plants at the vegetated plots is now oxidized in the soil, since now it has to slowly diffuse through the water phase. Thus, the fluxes measured at the clipped plots might not represent only the CH_4 that is transported via soil diffusion in the intact environment but account also for a part of CH_4 that is transported through the vegetation under natural conditions. On the other hand, the removal of the vegetation also ends the support for

CH_4 production by root exudates, limiting CH_4 production. These two contrary processes, whose effects on CH_4 fluxes were not quantified, introduce further uncertainties to our estimates.

We consider the difference between clipped and vegetated sites as a measure of the plant-mediated transport of CH_4 because there was no evidence of significant ebullitive transport at our sites. There was no abrupt increase in CH_4 concentrations during chamber closure times in any of our chamber measurements throughout the growing season (e.g., Figure S3 in Supporting Information S1), which would indicate ebullitive CH_4 fluxes. We presume that the dense root system of the vegetation at the polygon center prevented CH_4 to move through the water as bubbles. Although we cannot exclude the possibility of a small contribution of ebullitive CH_4 fluxes into the total CH_4 transported to the atmosphere, we consider that the linearity of CH_4 concentrations during chamber deployment in all our CH_4 chamber measurements demonstrate that the transport of CH_4 was overall comprised by plant-mediated and diffusive transport. Additionally, Knoblauch et al. (2015) have found negligible ebullitive fluxes in most of the studied polygon ponds on Samoylov Island, with similar soils as the one in this study.

At the polygon rim, we estimated a negligible plant-mediated transport of 3% similar to D. Wagner et al. (2003), while Kutzbach et al. (2004) detected 27%. However, the latter study also reported higher CH_4 fluxes at the rim and used a different approach to quantify plant-mediated transport that could be one of the causes for the distinct results: Kutzbach et al. (2004) used closed chambers that enclosed single *Carex aquatilis* culms, excluding CH_4 being transported by the soil. Ebullitive CH_4 fluxes were not observed at the polygon rim due to non-water-saturated conditions. The soil at the polygon rim in our study contained a deep oxic, unsaturated layer and released less CH_4 regardless of the removal of the vegetation. Presumably, both low CH_4 production and high CH_4 oxidation (Liebner & Wagner, 2007) affected the CH_4 release at the polygon rim simultaneously (Vaughn et al., 2016). Moreover, the polygon rim was mostly vegetated by mosses and small vascular plants (*Dryas punctata* and *Astragalus frigidus*) that do not possess aerenchyma like sedges. Hence, well-drained soil conditions, resulting in low CH_4 production and low presence of aerenchymatous plants are the likely reasons for only a small difference between CH_4 fluxes at the clipped and vegetated plots.

4.3. In situ CO_2:CH_4 Ratios and Their Environmental Controls

The rapid decrease of CO_2:CH_4 ratios at the polygon center from 94.6 to 12.5 between 11 July and 1 August shows the increasing relevance of the CH_4 production and decreased impact of R_h during the progression of the growing season. Methane fluxes increased from 5.8 to 21.5 mg m^{-2} d^{-1} in this period, following the deepening of the active layer. The negative relationship of the ALD with the CO_2:CH_4 ratios has also been demonstrated in previous studies (McCalley et al., 2014; van Huissteden et al., 2005). The reason for this relationship is an increase in the water-saturated, and hence anoxic, unfrozen soil volume (Lagomarsino & Agnelli, 2020; Rößger et al., 2022) but also the growth of vegetation, a consequence of increased substrate and nutrient availability with active layer thawing (Andresen et al., 2017).

In addition to ALD, soil temperature had a strong effect on CH_4 fluxes and CO_2:CH_4 ratios. Methane production is, as with any other microbial process, temperature-dependent (Y. Chen et al., 2022; Kelly & Chynoweth, 1981; Schädel et al., 2016; Treat et al., 2015; Zeikus & Winfrey, 1976; Zinder et al., 1984). Kolton et al. (2019) detected a negative relationship between temperature and CO_2:CH_4 ratios, indicating a stronger increase in CH_4 production with rising temperatures than CO_2 production. The production of CH_4 was directly correlated to rising soil temperatures at the depth of 40 cm, but also indirectly by promoting the deepening of the active layer. Similar results were reported by Rößger et al. (2022) in Samoylov Island, showing that polygon center soil temperature at 30 cm, thaw depth, and growing degree days were the variables with the highest CH_4 fluxes predictive power. In contrast, R_h at the center had only a weak relationship with the soil temperature at 40 cm depth. However, Eckhardt et al. (2019) identified air temperature followed by Surf$T$ as the best predictor for R_h at the polygon center. These observations indicate that CH_4 fluxes are affected by processes and changes happening at deeper soil layers (D. Wagner et al., 2003), while R_h is affected by processes in the top-soil (Ferréa et al., 2012). The deepest soil layer of our site was not affected by water table variations and maintained its anoxic conditions, enabling the establishment and active methanogenic community (Knoblauch et al., 2015; Liebner et al., 2015), while the soil surface contains the highest O_2 concentrations, staying frequently above the water table. An incubation experiment using samples from Samoylov Island presented evidence for the markedly higher methanogenesis potential of the bottom active layer compared to the surface (Walz et al., 2017). Therefore, the warming of the soil surface stimulates R_h, causing elevated CO_2:CH_4 ratios, while the warming of deeper anoxic soil layers,

stimulates methanogenesis and decreases the CO_2:CH_4 ratios. It might be expected that the surface and deep soil temperatures should be highly related, but just a weak relationship between SurfT and SoilT40 at the polygon center was detected in this study. The soil at the depth of 40 cm is in constant interaction with the underlying permafrost and remained frozen during about one third of the measurement period. The thermal regime at this depth is less controlled by solar radiation and more by the underlying permafrost temperatures than at the soil surface. The CO_2:CH_4 ratios at the polygon rim was governed mainly by the R_h variability since the CH_4 production is low throughout the measurement period. This is also demonstrated by the relationship between CO_2:CH_4 ratios at the rim and the SurfT, which was also the case for R_h.

The theoretical CO_2:CH_4 production ratio during anaerobic organic matter decomposition via methanogenesis is about 1 when the oxidation number of the organic matter is zero (Symons & Buswell, 1933). However, under natural conditions, CO_2:CH_4 ratios above one are generally reported even under anoxic conditions, since alternative electron acceptors such as nitrate, ferric iron, sulfate, or even organic matter may be used for SOM decomposition (Dettling et al., 2006). Anoxic incubations show a decrease in the CO_2:CH_4 ratios throughout the experiment, reaching values of about one, most likely because alternative electron acceptors get depleted and methanogenic communities become active (Knoblauch et al., 2018; Philben et al., 2020). The increase of CH_4 production with decreasing availability of alternative electron acceptors has been observed at other Arctic sites (Rissanen et al., 2017) and could have also played a role in the change of CO_2:CH_4 ratios in the current study. A shallow ALD at the beginning of the growing season results in a dominance of oxic organic matter decomposition in the oxic surface soil and a reoxidation of alternative electron acceptors. Later on, as the active layer keeps deepening, the anoxic bottom soil thaws and anoxic microbial organic matter decomposition becomes increasingly important, and with the depletion of the alternative electron acceptors, methanogenesis may increase. However, a ratio between CO_2 and CH_4 production above one is expected even under optimum conditions for methanogenesis in the anoxic soil at the polygon center, since CO_2 from heterotrophic respiration was predominantly formed in the oxic surface soil (see discussion above), where no CH_4 is produced.

4.4. In situ CO_2:CH_4 Production Ratios Uncertainty Range

While several methods are established to quantify microbial CO_2 production from SOM decomposition (R_h), the quantification of in situ CH_4 production is still challenging. The current study uses CO_2 fluxes from clipped plots to determine R_h fluxes (Eckhardt et al., 2019). To estimate in situ CH_4 production, the CH_4 fluxes above intact vegetation have been used before (Cooper et al., 2017). These CH_4 fluxes are the sum of CH_4 transported by aerenchymatous plants and by molecular diffusion through the soil and ebullition. This approach is likely underestimating in situ CH_4 production since a part of the produced CH_4 is oxidized in the soil before being emitted.

By using the fraction of oxidized CH_4 and the fraction of CH_4 diffusing through the soil from Knoblauch et al. (2015) and Preuss et al. (2013) we estimated that a fraction between 0.10 and 0.31 of produced CH_4 might have been oxidized in the soil before emitted into the atmosphere. Knoblauch et al. (2015) and Preuss et al. (2013) determined the fraction of oxidized CH_4 by using the δ^{13}C-values of CH_4 from rhizospheric and emitted CH_4. This method is based on the fact that isotopic fractionation occurs when CH_4 is oxidized during transport. Methanotrophs oxidize preferentially the lighter $^{12}CH_4$, leaving the heavier $^{13}CH_4$ behind. Our estimated fractions of 0.10–0.31 oxidized CH_4 are within in the range (0.01–0.40) reported by previous studies carried out in similar environments, including sites dominated by sedges of *Carex sp.* (Nielsen, Michelsen, Ambus, et al., 2017; Popp et al., 1999; Ström et al., 2005). This large range is both due to differences in the methodology to determine CH_4 oxidation in the soil but also due to differences in soil conditions and vegetation composition.

Methane oxidation is closely related to the efficiency of oxygen transport by the plant's roots, which is a species-specific characteristic (Nielsen, Michelsen, Ambus, et al., 2017), and seemingly a more important factor determining CH_4 oxidation than plant biomass (Ström et al., 2005). The contribution of CH_4 oxidation varies throughout ecosystems and vegetation composition. A study in a wetland in South Sweden identified that 20%–40% of produced CH_4 was oxidized in a *Carex rostrata*-dominated peat monolith, and more than 90% in monoliths with *Eriophorum vaginatum* (Ström et al., 2005), while in a southern Estonian bog, no significant CH_4 oxidation was found in an *Eriophorum spp.* dominated site (Frenzel & Rudolph, 1998). Thus, rhizospheric CH_4 oxidation regulated by the efficiency of oxygen transport by the plant's roots is apparently a site-specific characteristic in addition to being species-specific. Sedge species have been related to higher CH_4 fluxes than other plant species, not because they support CH_4 production but because they facilitate CH_4 transport through

their aerenchyma, bypassing the oxidative soil layer and avoiding oxidation (Green & Baird, 2012). Nielsen, Michelsen, Ambus, et al. (2017) showed in a wet tundra ecosystem in Greenland, that the radial oxygen loss of *Carex aquatilis* has a minor impact on CH_4 oxidation. In their study, the fraction of CH_4 oxidized was less than 2%, most likely because CH_4 diffusion is faster than it would be required for CH_4 oxidation and because CH_4 diffuses into plant roots at a lower depth than where oxidation takes place. Isotopic signatures of CH_4 from a bog in Stordalen Mire, Sweden, show a higher fraction of oxidized CH_4 occurring in periodically inundated shallower soil layers instead of permanently inundated deeper soil layers (Singleton et al., 2018). This is evidence of the latter hypothesis conceived by Nielsen, Michelsen, Ambus, et al. (2017) about the depth separation between the soil layers where CH_4 diffuses into plant roots and the region where CH_4 oxidation takes place.

Data from Samoylov Island, from a study on a similar polygon center, report no significant differences between the $\delta^{13}C$ signatures of dissolved CH_4 in the anoxic soil and of the emitted CH_4 from plots vegetated by *Carex aquatilis*, and hence give no evidence for rhizospheric CH_4 oxidation (Knoblauch et al., 2015). Since the vascular plants in our studied polygon were dominated by *C. aquatilis*, which was shown to only weakly support CH_4 oxidation in the rhizosphere, we consider that the calculated range of rhizospheric CH_4 oxidation (0.10—0.31) is rather at the higher end of CH_4 oxidation under in situ conditions and that the measured CH_4 fluxes in the polygon center are not severely affected by CH_4 oxidation. Due to the lack of estimates of the fraction of CH_4 oxidized at the polygon rim, low fluxes measured, low presence of aerenchymatous plants and oxic conditions, we could not calculate such a range of rhizospheric CH_4 oxidation as we did for the polygon center. Thus, we cannot consider the CO_2:CH_4 ratios as production ratios in the polygon rim.

4.5. Seasonal Heterotrophic Respiration and CH_4 fluxes

As expected, the wet tundra, which is water saturated, showed lower R_h fluxes, which were measured with the dark chambers in the clipped plots, while higher R_h fluxes were found in the dry tundra, and the opposite was the case for CH_4, which was measured with the transparent chambers in the vegetated plots. The dry tundra dominates total carbon fluxes, both due to high R_h and due to the larger area, since 185 ha is occupied by dry tundra and only 54.1 ha of the island is occupied by wet tundra (Muster et al., 2012). While both tundra types lost carbon preferentially in the form of R_h, CH_4-C represented 0.27% of the dry tundra total carbon flux and 6.91% of the wet tundra total carbon flux. The contribution of CH_4 fluxes to the seasonal R_h and CH_4 fluxes on Samoylov might change in the future. The ALD at Samoylov Island is predicted to increase (Beermann et al., 2017), as well as at several Arctic sites, related to increasing temperatures affecting the extension of the thawing period (Andresen et al., 2017; Euskirchen et al., 2006; Strand et al., 2021). This trend can be detected at Arctic sites in the past and today (Andresen et al., 2017; Strand et al., 2021). As shown in this study, the importance of CH_4 fluxes increases with increasing ALD depth. Our results are consistent with the study of Rößger et al. (2022) who also found a significant relationship between ALD and CH_4 fluxes and evidence for an increasing trend of early summer CH_4 fluxes from wet tundra linked to atmospheric warming. Moreover, to predict the future response of CH_4 fluxes from thawing permafrost landscapes it will be crucial to understand if the ALD increase will result in wetter soils (Krogh & Pomeroy, 2019), thereby increasing CH_4 fluxes (Tagesson et al., 2012) or drier soils (Jin et al., 2021; Natali et al., 2015) resulting in lower CH_4 fluxes (Kim, 2015).

5. Conclusions

Methane fluxes presented here are at the lower end compared to other Arctic sites, and the differences found between these fluxes and the ones from other measurements in Samoylov Island show the high temporal and spatial variability found in GHG fluxes in the Siberian tundra. Understanding the mechanisms that control the CO_2:CH_4 production ratios is especially important for improving Earth System models. To estimate the CO_2:CH_4 production ratios under in situ conditions we used the R_h fluxes from clipped plots and the CH_4 fluxes from vegetated plots, which were corrected for potential CH_4 oxidation in the soil. The CO_2:CH_4 production ratio is associated with active-layer depth (ALD) due to a direct effect of ALD on methane production. The effect of air temperature seasonality on the CO_2:CH_4 ratio is complicated. Topsoil (5 cm) warming stimulates heterotrophic respiration under more oxic conditions, hence increasing the CO_2:CH_4 ratio. In contrast, warming of anoxic subsoil (40 cm) layers leads to enhanced CH_4 production, hence a lowering of the CO_2:CH_4 ratio.

Arctic warming will lead to a warming of the active layer and its deepening. Our study indicates that for wet tundra this warming and deepening can result in a pronounced rise in CH_4 production. Changing vegetation

patterns and functions, however, will further convolute the net response of Arctic CH_4 fluxes to global warming. Further studies are needed focusing on the complexities of in situ CH_4 and CO_2 production, especially in regions where there is yet scarcity of data, like the vast Siberian tundra. There is still a high uncertainty on the response of CH_4 production and fluxes to thawing permafrost and the related feedback mechanism.

Data Availability Statement

The chamber methane fluxes and active layer depths data are available at PANGAEA via https://doi.pangaea.de/10.1594/PANGAEA.944841 with Creative Commons Attribution 4.0 International (CC-BY-4.0) (Galera et al., 2022a). The in situ CO_2:CH_4 production ratios data are available at PANGAEA via https://doi.pangaea.de/10.1594/PANGAEA.944844 with CC-BY-4.0 (Galera et al., 2022b).

References

Andresen, C. G., Lara, M. J., Tweedie, C. E., & Lougheed, V. L. (2017). Rising plant-mediated methane emissions from arctic wetlands. *Global Change Biology*, *23*(3), 1128–1139. https://doi.org/10.1111/gcb.13469

Bastviken, D., Cole, J. J., Pace, M. L., & Van de-Bogert, M. C. (2008). Fates of methane from different lake habitats: Connecting whole-lake budgets and CH_4 emissions. *Journal of Geophysical Research*, *113*(2), 1–13. https://doi.org/10.1029/2007JG000608

Beckebanze, L., Rehder, Z., Holl, D., Wille, C., Mirbach, C., & Kutzbach, L. (2022). Ignoring carbon emissions from thermokarst ponds results in overestimation of tundra net carbon uptake. *Biogeosciences*, *19*(4), 1225–1244. https://doi.org/10.5194/bg-19-1225-2022

Beckebanze, L., Runkle, B. R. K., Walz, J., Wille, C., Holl, D., Helbig, M., et al. (2022). Lateral carbon export has low impact on the net ecosystem carbon balance of a polygonal tundra catchment. *Biogeosciences*, *19*(16), 3863–3876. https://doi.org/10.5194/bg-19-3863-2022

Beermann, F., Langer, M., Wetterich, S., Strauss, J., Boike, J., Fiencke, C., et al. (2017). Permafrost thaw and liberation of inorganic nitrogen in eastern Siberia. *Permafrost and Periglacial Processes*, *28*(4), 605–618. https://doi.org/10.1002/ppp.1958

Biskaborn, B. K., Smith, S. L., Noetzli, J., Matthes, H., Vieira, G., Streletskiy, D. A., et al. (2019). Permafrost is warming at a global scale. *Nature Communications*, *10*(1), 264. https://doi.org/10.1038/s41467-018-08240-4

Bodegom, P. M. V., & Stams, A. J. M. (1999). Effects of alternative electron acceptors and temperature on methanogenesis in rice paddy soils. *Chemosphere*, *39*(2), 167–182. https://doi.org/10.1016/S0045-6535(99)00101-0

Boike, J., Grüber, M., Langer, M., Piel, K., & Scheritz, M. (2012). *Orthomosaic of Samoylov Island, Lena Delta, Siberia*. PANGAEA. https://doi.org/10.1594/PANGAEA.786073

Boike, J., Kattenstroth, B., Abramova, K., Bornemann, N., Chetverova, A., Fedorova, I., et al. (2013). Baseline characteristics of climate, permafrost and land cover from a new permafrost observatory in the Lena River Delta, Siberia (1998-2011). *Biogeosciences*, *10*(3), 2105–2128. https://doi.org/10.5194/bg-10-2105-2013

Boike, J., Nitzbon, J., Anders, K., Grigoriev, M., Bolshiyanov, D., Langer, M., et al. (2019). A 16-year record (2002--2017) of permafrost, active-layer, and meteorological conditions at the Samoylov Island Arctic permafrost research site, Lena River Delta, northern Siberia: An opportunity to validate remote-sensing data and land surface, snow, and permafrost models. *Earth System Science Data*, *11*(1), 261–299. https://doi.org/10.5194/essd-11-261-2019

Boike, J., Veh, G., Viitanen, L.-K., Bornemann, N., Stoof, G. n., & Muster, S. (2015). *Visible and near-infrared orthomosaic of Samoylov Island, Siberia, summer 2015 (5.3 GB)*. PANGAEA. https://doi.org/10.1594/PANGAEA.845724

Cannone, N., Augusti, A., Malfasi, F., Pallozzi, E., Calfapietra, C., & Brugnoli, E. (2016). The interaction of biotic and abiotic factors at multiple spatial scales affects the variability of CO2 fluxes in polar environments. *Polar Biology*, *39*(9), 1581–1596. https://doi.org/10.1007/s00300-015-1883-9

Chen, W., Wolf, B., Zheng, X., Yao, Z., Butterbach-Bahl, K., Brüggemann, N., et al. (2011). Annual methane uptake by temperate semiarid steppes as regulated by stocking rates, aboveground plant biomass and topsoil air permeability. *Global Change Biology*, *17*(9), 2803–2816. https://doi.org/10.1111/j.1365-2486.2011.02444.x

Chen, Y., Wu, N., Liu, C., Mi, T., Li, J., He, X., et al. (2022). Methanogenesis pathways of methanogens and their responses to substrates and temperature in sediments from the South Yellow Sea. *Science of the Total Environment*, *815*, 152645. https://doi.org/10.1016/j.scitotenv.2021.152645

Christiansen, J. R., Korhonen, J. F. J., Juszczak, R., Giebels, M., & Pihlatie, M. (2011). Assessing the effects of chamber placement, manual sampling and headspace mixing on CH_4 fluxes in a laboratory experiment. *Plant and Soil*, *343*(1), 171–185. https://doi.org/10.1007/s11104-010-0701-y

Christiansen, J. R., Romero, A. J. B., Jørgensen, N. O. G., Glaring, M. A., Jørgensen, C. J., Berg, L. K., & Elberling, B. (2015). Methane fluxes and the functional groups of methanotrophs and methanogens in a young Arctic landscape on Disko Island, West Greenland. *Biogeochemistry*, *122*(1), 15–33. https://doi.org/10.1007/s10533-014-0026-7

Clymo, R. S., & Bryant, C. L. (2008). Diffusion and mass flow of dissolved carbon dioxide, methane, and dissolved organic carbon in a 7-m deep raised peat bog. *Geochimica et Cosmochimica Acta*, *72*(8), 2048–2066. https://doi.org/10.1016/j.gca.2008.01.032

Clymo, R. S., Pearce, D. M. E., & Conrad, R. (1995). Methane and carbon dioxide production in, transport through, and efflux from a peatland [and discussion]. *Philosophical Transactions: Physical Sciences and Engineering*, *351*(1696), 249–259. Retrieved from http://www.jstor.org/stable/54414

Cooper, M. D. A., Estop-Aragonés, C., Fisher, J. P., Thierry, A., Garnett, M. H., Charman, D. J., et al. (2017). Limited contribution of permafrost carbon to methane release from thawing peatlands. *Nature Climate Change*, *7*(7), 507–511. https://doi.org/10.1038/nclimate3328

Delwiche, K. B., Knox, S. H., Malhotra, A., Fluet-Chouinard, E., McNicol, G., Feron, S., et al. (2021). FLUXNET-CH4: A global, multi-ecosystem dataset and analysis of methane seasonality from freshwater wetlands. *Earth System Science Data*, *13*(7), 3607–3689. https://doi.org/10.5194/essd-13-3607-2021

Dettling, M. D., Yavitt, J. B., & Zinder, S. H. (2006). Control of organic carbon mineralization by alternative electron acceptors in four peatlands, Central New York State, USA. *Wetlands*, *26*(4), 917–927. https://doi.org/10.1672/0277-5212(2006)26[917:COOCMB]2.0.CO;2

Eckhardt, T., Knoblauch, C., Kutzbach, L., Holl, D., Simpson, G., Abakumov, E., & Pfeiffer, E. M. (2019). Partitioning net ecosystem exchange of CO_2 on the pedon scale in the Lena River Delta, Siberia. *Biogeosciences*, *16*(7), 1543–1562. https://doi.org/10.5194/bg-16-1543-2019

Eckhardt, T., & Kutzbach, L. (2016). *MATLAB code to calculate gas fluxes from chamber-based methods*. PANGAEA. https://doi.pangaea.de/10.1594/PANGAEA.857799

Euskirchen, E. S., Bret-Harte, M. S., Shaver, G. R., Edgar, C. W., & Romanovsky, V. E. (2017). Long-term release of carbon dioxide from arctic tundra ecosystems in Alaska. *Ecosystems*, *20*(5), 960–974. https://doi.org/10.1007/s10021-016-0085-9

Euskirchen, E. S., McGuire, A. D., Kicklighter, D. W., Zhuang, Q., Clein, J. S., Dargaville, R. J., et al. (2006). Importance of recent shifts in soil thermal dynamics on growing season length, productivity, and carbon sequestration in terrestrial high-latitude ecosystems. *Global Change Biology*, *12*(4), 731–750. https://doi.org/10.1111/j.1365-2486.2006.01113.x

Ferréa, C., Zenone, T., Comolli, R., & Seufert, G. (2012). Estimating heterotrophic and autotrophic soil respiration in a semi-natural forest of Lombardy, Italy. *Pedobiologia*, *55*(6), 285–294. https://doi.org/10.1016/j.pedobi.2012.05.001

Frenzel, P., & Rudolph, J. (1998). Methane emission from a wetland plant: The role of CH_4 oxidation in Eriophorum. *Plant and Soil*, *202*(1), 27–32. https://doi.org/10.1023/a:1004348929219

Galera, L. D. A., Eckhardt, T., Beer, C., Pfeiffer, E.-M., Kutzbach, L., Simpson, G., et al. (2022a). Chamber methane fluxes and active layer depths from a polygon in northeastern Siberia [Dataset]. PANGAEA. https://doi.org/10.1594/PANGAEA.944841

Galera, L. D. A., Eckhardt, T., Beer, C., Pfeiffer, E.-M., Kutzbach, L., Simpson, G., et al. (2022b). In situ CO_2/CH_4 production ratios from a polygon in northeastern Siberia [Dataset]. PANGAEA. https://doi.org/10.1594/PANGAEA.944844

Girkin, N. T., Turner, B. L., Ostle, N., Craigon, J., & Sjögersten, S. (2018). Root exudate analogues accelerate CO_2 and CH_4 production in tropical peat. *Soil Biology and Biochemistry*, *117*, 48–55. https://doi.org/10.1016/j.soilbio.2017.11.008

Google Earth 9.185.0.0. Eurasia. 51°21'20"N, 63°44'44"E, Camera 12,840 km. Landsat/Copernicus. Data SIO, NOAA, U.S. Navy, NGA, GEBCO, IBCAO, U.S. Geological Survey, INEGI. (Acessed February 27, 2023).

Green, S. M., & Baird, A. J. (2012). A mesocosm study of the role of the sedge Eriophorum angustifolium in the efflux of methane-including that due to episodic ebullition-from peatlands. *Plant and Soil*, *351*(1–2), 207–218. https://doi.org/10.1007/s11104-011-0945-1

Heslop, J. K., Winkel, M., Walter Anthony, K. M., Spencer, R. G. M., Podgorski, D. C., Zito, P., et al. (2019). Increasing organic carbon biolability with depth in Yedoma permafrost: Ramifications for future climate change. *Journal of Geophysical Research: Biogeosciences*, *124*(7), 2021–2038. https://doi.org/10.1029/2018JG004712

IPCC. (2022). Summary for policymakers. In H.-O., Pörtner, D.C., Roberts, E.S., Poloczanska, K., Mintenbeck, M., Tignor, et al. (Eds.), *Climate Change 2022: Impacts, Adaptation and Vulnerability. Contribution of Working Group II to the Sixth Assessment Report of the Intergovernmental Panel on climate change* (pp. 3–33). Cambridge University Press. https://doi.org/10.1017/9781009325844.001

Jin, X.-Y., Jin, H.-J., Iwahana, G., Marchenko, S. S., Luo, D.-L., Li, X.-Y., & Liang, S.-H. (2021). Impacts of climate-induced permafrost degradation on vegetation: A review. *Advances in Climate Change Research*, *12*(1), 29–47. https://doi.org/10.1016/j.accre.2020.07.002

Joabsson, A., & Christensen, T. R. (2001). Methane emissions from wetlands and their relationship with vascular plants: An Arctic example. *Global Change Biology*, *7*(8), 919–932. https://doi.org/10.1046/j.1354-1013.2001.00044.x

Jørgensen, C. J., Johansen, K. M. L., Westergaard-Nielsen, A., Elberling, B., Juncher Jørgensen, C., Lund Johansen, K. M., et al. (2015). Net regional methane sink in High Arctic soils of northeast Greenland. *Nature Geoscience*, *8*(1), 20–23. https://doi.org/10.1038/ngeo2305

Kelly, C. A., & Chynoweth, D. P. (1981). The contributions of temperature and of the input of organic matter in controlling rates of sediment methanogenesis1. *Limnology & Oceanography*, *26*(5), 891–897. https://doi.org/10.4319/lo.1981.26.5.0891

Khokhar, N. H., & Park, J.-W. (2017). A simplified sampling procedure for the estimation of methane emission in rice fields. *Environmental Monitoring and Assessment*, *189*(9), 468. https://doi.org/10.1007/s10661-017-6184-z

Kim, Y. (2015). Effect of thaw depth on fluxes of CO_2 and CH_4 in manipulated Arctic coastal tundra of Barrow, Alaska. *Science of the Total Environment*, *505*, 385–389. https://doi.org/10.1016/j.scitotenv.2014.09.046

Kleinen, T., Gromov, S., Steil, B., & Brovkin, V. (2021). Atmospheric methane underestimated in future climate projections. *Environmental Research Letters*, *16*(9), 094006. https://doi.org/10.1088/1748-9326/ac1814

Knoblauch, C., Beer, C., Liebner, S., Grigoriev, M. N., & Pfeiffer, E. M. (2018). Methane production as key to the greenhouse gas budget of thawing permafrost. *Nature Climate Change*, *8*(April), 1–4. https://doi.org/10.1038/s41558-018-0095-z

Knoblauch, C., Spott, O., Evgrafova, S., Kutzbach, L., & Pfeiffer, E. M. (2015). Regulation of methane production, oxidation, and emission by vascular plants and bryophytes in ponds of the northeast Siberian polygonal tundra. *Journal of Geophysical Research: Biogeosciences*, *120*(12), 2525–2541. https://doi.org/10.1002/2015JG003053

Kolton, M., Marks, A., Wilson, R. M., Chanton, J. P., & Kostka, J. E. (2019). Impact of warming on greenhouse gas production and microbial diversity in anoxic peat from a sphagnum-dominated bog (Grand Rapids, Minnesota, United States). *Frontiers in Microbiology*, *10*, 870. https://doi.org/10.3389/fmicb.2019.00870

Krauss, K. W., Holm Jr., G. O., Perez, B. C., McWhorter, D. E., Cormier, N., Moss, R. F., et al. (2016). Component greenhouse gas fluxes and radiative balance from two deltaic marshes in Louisiana: Pairing chamber techniques and eddy covariance. *Journal of Geophysical Research: Biogeosciences*, *121*(6), 1503–1521. https://doi.org/10.1002/2015JG003224

Krogh, S. A., & Pomeroy, J. W. (2019). Impact of future climate and vegetation on the hydrology of an arctic headwater basin at the tundra–taiga transition. *Journal of Hydrometeorology*, *20*(2), 197–215. https://doi.org/10.1175/JHM-D-18-0187.1

Kutzbach, L., Wagner, D., & Pfeiffer, E. M. (2004). Effect of microrelief and vegetation on methane emission from wet polygonal tundra, Lena Delta, Northern Siberia. *Biogeochemistry*, *69*(3), 341–362. https://doi.org/10.1023/B:BIOG.0000031053.81520.db

Kwon, M. J., Beulig, F., Ilie, I., Wildner, M., Küsel, K., Merbold, L., et al. (2017). Plants, microorganisms, and soil temperatures contribute to a decrease in methane fluxes on a drained Arctic floodplain. *Global Change Biology*, *23*(6), 2396–2412. https://doi.org/10.1111/gcb.13558

Lagomarsino, A., & Agnelli, A. E. (2020). Influence of vegetation cover and soil features on CO2, CH4 and N2O fluxes in northern Finnish Lapland. *Polar Science*, *24*, 100531. https://doi.org/10.1016/j.polar.2020.100531

Liebner, S., Ganzert, L., Kiss, A., Yang, S., Wagner, D., & Svenning, M. M. (2015). Shifts in methanogenic community composition and methane fluxes along the degradation of discontinuous permafrost. *Frontiers in Microbiology*, *6*, 356. https://doi.org/10.3389/fmicb.2015.00356

Liebner, S., & Wagner, D. (2007). Abundance, distribution and potential activity of methane oxidizing bacteria in permafrost soils from the Lena Delta, Siberia. *Environmental Microbiology*, *9*(1), 107–117. https://doi.org/10.1111/j.1462-2920.2006.01120.x

Lindroth, A., Pirk, N., Jónsdóttir, I. S., Stiegler, C., Klemedtsson, L., & Nilsson, M. B. (2022). CO2 and CH4 exchanges between moist moss tundra and atmosphere on Kapp Linné, Svalbard. *Biogeosciences*, *19*(16), 3921–3934. https://doi.org/10.5194/bg-19-3921-2022

Mastepanov, M., Sigsgaard, C., Dlugokencky, E. J., Houweling, S., Ström, L., Tamstorf, M. P., & Christensen, T. R. (2008). Large tundra methane burst during onset of freezing. *Nature*, *456*(7222), 628–630. https://doi.org/10.1038/nature07464

Mastepanov, M., Sigsgaard, C., Tagesson, T., Ström, L., Tamstorf, M. P., Lund, M., & Christensen, T. R. (2013). Revisiting factors controlling methane emissions from high-Arctic tundra. *Biogeosciences*, *10*(11), 5139–5158. https://doi.org/10.5194/bg-10-5139-2013

McCalley, C. K., Woodcroft, B. J., Hodgkins, S. B., Wehr, R. A., Kim, E. H., Mondav, R., et al. (2014). Methane dynamics regulated by microbial community response to permafrost thaw. *Nature*, *514*(7253), 478–481. https://doi.org/10.1038/nature13798

Melton, J. R., Wania, R., Hodson, E. L., Poulter, B., Ringeval, B., Spahni, R., et al. (2013). Present state of global wetland extent and wetland methane modelling: Conclusions from a model inter-comparison project (WETCHIMP). *Biogeosciences*, *10*(2), 753–788. https://doi.org/10.5194/bg-10-753-2013

Miner, K. R., Turetsky, M. R., Malina, E., Bartsch, A., Tamminen, J., McGuire, A. D., et al. (2022). Permafrost carbon emissions in a changing Arctic. *Nature Reviews Earth & Environment*, *3*(1), 55–67. https://doi.org/10.1038/s43017-021-00230-3

Mishra, U., Hugelius, G., Shelef, E., Yang, Y., Strauss, J., Lupachev, A., et al. (2021). Spatial heterogeneity and environmental predictors of permafrost region soil organic carbon stocks. *Science Advances*, *7*(9). eaaz5236-eaaz5236. https://doi.org/10.1126/sciadv.aaz5236

Morrissey, L. A., & Livingston, G. P. (1992). Methane emissions from Alaska Arctic tundra - an assessment of local spatial variability (Vol. *97*). https://doi.org/10.1029/92JD00063

Muster, S., Langer, M., Heim, B., Westermann, S., & Boike, J. (2012). Subpixel heterogeneity of ice-wedge polygonal tundra: A multi-scale analysis of land cover and evapotranspiration in the Lena River Delta, Siberia. *Tellus B: Chemical and Physical Meteorology*, *64*(1), 17301. https://doi.org/10.3402/tellusb.v64i0.17301

Myhre, G., Samset, B. H., Schulz, M., Balkanski, Y., Bauer, S., Berntsen, T. K., et al. (2013). Radiative forcing of the direct aerosol effect from AeroCom Phase II simulations. *Atmospheric Chemistry and Physics*, *13*(4), 1853–1877. https://doi.org/10.5194/acp-13-1853-2013

Natali, S. M., Schuur, E. A. G., Mauritz, M., Schade, J. D., Celis, G., Crummer, K. G., et al. (2015). Permafrost thaw and soil moisture driving CO_2 and CH_4 release from upland tundra. *Journal of Geophysical Research: Biogeosciences*, *120*(3), 525–537. https://doi.org/10.1002/2014JG002872

Natchimuthu, S., Wallin, M. B., Klemedtsson, L., & Bastviken, D. (2017). Spatio-temporal patterns of stream methane and carbon dioxide emissions in a hemiboreal catchment in Southwest Sweden. *Scientific Reports*, *7*(1), 39729. https://doi.org/10.1038/srep39729

Nielsen, C. S., Michelsen, A., Ambus, P., Deepagoda, T. K. K. C., & Elberling, B. (2017). Linking rhizospheric CH_4 oxidation and net CH_4 emissions in an arctic wetland based on 13CH_4 labeling of mesocosms. *Plant and Soil*, *412*(1–2), 201–213. https://doi.org/10.1007/s11104-016-3061-4

Nielsen, C. S., Michelsen, A., Strobel, B. W., Wulff, K., Banyasz, I., & Elberling, B. (2017). Correlations between substrate availability, dissolved CH_4, and CH_4 emissions in an arctic wetland subject to warming and plant removal. *Journal of Geophysical Research: Biogeosciences*, *122*(3), 645–660. https://doi.org/10.1002/2016JG003511

Noyce, G. L., Varner, R. K., Bubier, J. L., & Frolking, S. (2014). Effect of Carex rostrata on seasonal and interannual variability in peatland methane emissions. *Journal of Geophysical Research: Biogeosciences*, *119*(1), 24–34. https://doi.org/10.1002/2013JG002474

Philben, M., Zhang, L., Yang, Z., Taş, N., Wullschleger, S. D., Graham, D. E., & Gu, B. (2020). Anaerobic respiration pathways and response to increased substrate availability of Arctic wetland soils. *Environmental Sciences: Processes & Impacts*, *22*(10), 2070–2083. https://doi.org/10.1039/D0EM00124D

Pickett-Heaps, C. A., Jacob, D. J., Wecht, K. J., Kort, E. A., Wofsy, S. C., Diskin, G. S., et al. (2011). Magnitude and seasonality of wetland methane emissions from the Hudson Bay Lowlands (Canada). *Atmospheric Chemistry and Physics*, *11*(8), 3773–3779. https://doi.org/10.5194/acp-11-3773-2011

Pirk, N., Santos, T., Gustafson, C., Johansson, A. J., Tufvesson, F., Parmentier, F.-J. W., et al. (2015). Methane emission bursts from permafrost environments during autumn freeze-in: New insights from ground-penetrating radar. *Geophysical Research Letters*, *42*(16), 6732–6738. https://doi.org/10.1002/2015GL065034

Popp, T. J., Chanton, J. P., Whiting, G. J., & Grant, N. (1999). Methane stable isotope distribution at a Carex dominated fenin north Central Alberta. *Global Biogeochemical Cycles*, *13*(4), 1063–1077. https://doi.org/10.1029/1999GB900060

Popp, T. J., Chanton, J. P., Whiting, G. J., & Grant, N. (2000). Evaluation of methane oxidation in therhizosphere of a Carex dominated fen in northcentral Alberta, Canada. *Biogeochemistry*, *51*(3), 259–281. https://doi.org/10.1023/A:1006452609284

Preuss, I., Knoblauch, C., Gebert, J., & Pfeiffer, E. M. (2013). Improved quantification of microbial CH_4 oxidation efficiency in arctic wetland soils using carbon isotope fractionation. *Biogeosciences*, *10*(4), 2539–2552. https://doi.org/10.5194/bg-10-2539-2013

R. (2020). R: A language and environment for statistical computing. In *R Foundation for statistical computing*. Retrieved from https://www.R-project.org/

Rissanen, A. J., Karvinen, A., Nykänen, H., Peura, S., Tiirola, M., Mäki, A., & Kankaala, P. (2017). Effects of alternative electron acceptors on the activity and community structure of methane-producing and consuming microbes in the sediments of two shallow boreal lakes. *FEMS Microbiology Ecology*, *93*(7). https://doi.org/10.1093/femsec/fix078

Romanovsky, V. E., Smith, S. L., & Christiansen, H. H. (2010). Permafrost thermal state in the polar Northern Hemisphere during the international polar year 2007–2009: A synthesis. *Permafrost and Periglacial Processes*, *21*(2), 106–116. https://doi.org/10.1002/ppp.689

Rößger, N., Sachs, T., Wille, C., Boike, J., & Kutzbach, L. (2022). Seasonal increase of methane emissions linked to warming in Siberian tundra. *Nature Climate Change*, *12*(11), 1031–1036. https://doi.org/10.1038/s41558-022-01512-4

Sachs, T., Giebels, M., Boike, J., & Kutzbach, L. (2010). Environmental controls on CH_4 emission from polygonal tundra on the microsite scale in the Lena river delta, Siberia. *Global Change Biology*, *16*(11), 3096–3110. https://doi.org/10.1111/j.1365-2486.2010.02232.x

Saunois, M., Stavert, A. R., Poulter, B., Bousquet, P., Canadell, J. G., Jackson, R. B., et al. (2020). The global methane budget 2000–2017. *Earth System Science Data*, *12*(3), 1561–1623. https://doi.org/10.5194/essd-12-1561-2020

Schädel, C., Bader, M. K. F., Schuur, E. A. G., Biasi, C., Bracho, R., Čapek, P., et al. (2016). Potential carbon emissions dominated by carbon dioxide from thawed permafrost soils. *Nature Climate Change*, *6*(10), 950–953. https://doi.org/10.1038/nclimate3054

Schrier-Uijl, A. P., Kroon, P. S., Hensen, A., Leffelaar, P. A., Berendse, F., & Veenendaal, E. M. (2010). Comparison of chamber and eddy covariance-based CO_2 and CH_4 emission estimates in a heterogeneous grass ecosystem on peat. *Agricultural and Forest Meteorology*, *150*(6), 825–831. https://doi.org/10.1016/j.agrformet.2009.11.007

Schuur, E. A. G., McGuire, A. D., Schädel, C., Grosse, G., Harden, J. W., Hayes, D. J., et al. (2015). Climate change and the permafrost carbon feedback. *Nature*, *520*(7546), 171–179. https://doi.org/10.1038/nature14338

Singh, A., & Chaturvedi, P. (2021). Error Propagation. *Resonance*, *26*(6), 853–861. https://doi.org/10.1007/s12045-021-1185-1

Singleton, C. M., McCalley, C. K., Woodcroft, B. J., Boyd, J. A., Evans, P. N., Hodgkins, S. B., et al. (2018). Methanotrophy across a natural permafrost thaw environment. *The ISME Journal*, *12*(10), 2544–2558. https://doi.org/10.1038/s41396-018-0065-5

Skeeter, J., Christen, A., Laforce, A.-A., Humphreys, E., & Henry, G. (2020). Vegetation influence and environmental controls on greenhouse gas fluxes from a drained thermokarst lake in the Western Canadian Arctic. *Biogeosciences Discussions*, *17*, 1–25. https://doi.org/10.5194/bg-2019-477

St Pierre, K. A., Danielsen, B. K., Hermesdorf, L., D'Imperio, L., Iversen, L. L., & Elberling, B. (2019). Drivers of net methane uptake across Greenlandic dry heath tundra landscapes. *Soil Biology and Biochemistry*, *138*, 107605. https://doi.org/10.1016/j.soilbio.2019.107605

Strand, S. M., Christiansen, H. H., Johansson, M., Åkerman, J., & Humlum, O. (2021). Active layer thickening and controls on interannual variability in the Nordic Arctic compared to the circum-Arctic. *Permafrost and Periglacial Processes*, *32*(1), 47–58. https://doi.org/10.1002/ppp.2088

Ström, L., Mastepanov, M., & Christensen, T. R. (2005). Species-specific effects of vascular plants on carbon turnover and methane emissions from wetlands. *Biogeochemistry*, *75*(1), 65–82. https://doi.org/10.1007/s10533-004-6124-1

Ström, L., Tagesson, T., Mastepanov, M., & Christensen, T. R. (2012). Presence of Eriophorum scheuchzeri enhances substrate availability and methane emission in an Arctic wetland. *Soil Biology and Biochemistry*, *45*, 61–70. https://doi.org/10.1016/j.soilbio.2011.09.005

Symons, G. E., & Buswell, A. M. (1933). The methane fermentation of carbohydrates 1,2. *Journal of the American Chemical Society*, *55*(5), 2028–2036. https://doi.org/10.1021/ja01332a039

Tagesson, T., Mölder, M., Mastepanov, M., Sigsgaard, C., Tamstorf, M. P., Lund, M., et al. (2012). Land-atmosphere exchange of methane from soil thawing to soil freezing in a high-Arctic wet tundra ecosystem. *Global Change Biology*, *18*(6), 1928–1940. https://doi.org/10.1111/j.1365-2486.2012.02647.x

Treat, C. C., Natali, S. M., Ernakovich, J., Iversen, C. M., Lupascu, M., McGuire, A. D., et al. (2015). A pan-Arctic synthesis of CH_4 and CO_2 production from anoxic soil incubations. *Global Change Biology*, *21*(7), 2787–2803. https://doi.org/10.1111/gcb.12875

Treat, C. C., Wollheim, W. M., Varner, R. K., Grandy, A. S., Talbot, J., & Frolking, S. (2014). Temperature and peat type control CO_2 and CH_4 production in Alaskan permafrost peats. *Global Change Biology*, *20*(8), 2674–2686. https://doi.org/10.1111/gcb.12572

van Huissteden, J. (2020). *Thawing permafrost: Permafrost carbon in a warming Arctic* (1 ed.). Springer Nature Switzerland AG. https://doi.org/10.1007/978-3-030-31379-1

van Huissteden, J., Maximov, T. C., & Dolman, A. J. (2005). High methane flux from an arctic floodplain (Indigirka lowlands, eastern Siberia). *Journal of Geophysical Research*, *110*(G2). https://doi.org/10.1029/2005JG000010

Vasiliev, A. A., Melnikov, V. P., Semenov, P. B., Oblogov, G. E., & Streletskaya, I. D. (2019). Methane concentration and emission in dominant landscapes of typical tundra of Western Yamal. *Doklady Earth Sciences*, *485*(1), 284–287. https://doi.org/10.1134/S1028334X19030085

Vaughn, L. J. S., Conrad, M. E., Bill, M., & Torn, M. S. (2016). Isotopic insights into methane production, oxidation, and emissions in Arctic polygon tundra. *Global Change Biology*, *22*(10), 3487–3502. https://doi.org/10.1111/gcb.13281

Wagner, D., Kobabe, S., Pfeiffer, E. M., & Hubberten, H. W. (2003). Microbial controls on methane fluxes from a polygonal tundra of the Lena Delta, Siberia. *Permafrost and Periglacial Processes*, *14*(3), 173–185. https://doi.org/10.1002/ppp.443

Wagner, I., Hung, J. K. Y., Neil, A., & Scott, N. A. (2019). Net greenhouse gas fluxes from three High Arctic plant communities along a moisture gradient. *Arctic Science*, *5*(June), 185–201. https://doi.org/10.1139/as-2018-0018

Walz, J., Knoblauch, C., Böhme, L., & Pfeiffer, E.-M. (2017). Regulation of soil organic matter decomposition in permafrost-affected Siberian tundra soils - Impact of oxygen availability, freezing and thawing, temperature, and labile organic matter. *Soil Biology and Biochemistry*, *110*, 34–43. https://doi.org/10.1016/j.soilbio.2017.03.001

Wania, R., Ross, I., & Prentice, I. C. (2010). Implementation and evaluation of a new methane model within a dynamic global vegetation model: LPJ-WHyMe v1.3.1. *Geoscientific Model Development*, *3*(2), 565–584. https://doi.org/10.5194/gmd-3-565-2010

Whalen, S. C. (2005). Natural wetlands and the atmosphere. *Environmental Engineering Science*, *22*(1), 73–94. https://doi.org/10.1089/ees.2005.22.73

Wickland, K. P., Striegl, R. G., Neff, J. C., & Sachs, T. (2006). Effects of permafrost melting on CO_2 and CH_4 exchange of a poorly drained black spruce lowland. *Journal of Geophysical Research*, *111*(G2). https://doi.org/10.1029/2005JG000099

Wilber, A. C., Kratz, D. P., & Gupta, S. K. (1999). Surface emissivity maps for use in satellite retrievals of longwave radiation.

WRB, I. W. G. (2015). World reference base for soil resources 2014: International soil classification system for naming soils and creating legends for soil maps.

Yershov, E. D. (1998). *General geocryology*. Cambridge University Press. https://doi.org/10.1017/CBO9780511564505

Yvon-Durocher, G., Allen, A. P., Bastviken, D., Conrad, R., Gudasz, C., St-Pierre, A., et al. (2014). Methane fluxes show consistent temperature dependence across microbial to ecosystem scales. *Nature*, *507*(7493), 488–491. https://doi.org/10.1038/nature13164

Zeikus, J. G., & Winfrey, M. R. (1976). Temperature limitation of methanogenesis in aquatic sediments. *Applied and Environmental Microbiology*, *31*(1), 99–107. https://doi.org/10.1128/aem.31.1.99-107.1976

Zinder, S. H., Anguish, T., & Cardwell, S. C. (1984). Effects of temperature on methanogenesis in a thermophilic (58°C) anaerobic digestor. *Applied and Environmental Microbiology*, *47*(4), 808–813. https://doi.org/10.1128/aem.47.4.808-813.1984

Zona, D., Gioli, B., Commane, R., Lindaas, J., Wofsy, S. C., Miller, C. E., et al. (2016). Cold season emissions dominate the Arctic tundra methane budget. *Proceedings of the National Academy of Sciences*, *113*(1), 40–45. https://doi.org/10.1073/pnas.1516017113

Zubrzycki, S., Kutzbach, L., Grosse, G., Desyatkin, A., & Pfeiffer, E. M. (2013). Organic carbon and total nitrogen stocks in soils of the Lena River Delta. *Biogeosciences*, *10*(6), 3507–3524. https://doi.org/10.5194/bg-10-3507-2013